

# Degradation of Polymer Solar Cells: Knowledge Learned from the Polymer:Fullerene Solar Cells

Lingpeng Yan\* and Chang-Qi Ma\*

Although power conversion efficiency (PCE) of polymer solar cells (PSCs) has exceeded 18%, the lifetime of PSCs is far away from satisfactory and has become the most critical issue before the commercialization of PSCs. Understanding the degradation mechanism and finding the proper way to suppress the degradation process are of high interests for PSC research. Polymer:fullerene solar cells (PFSCs) have a long research history and the working principle is well-understood, so they are good models for the degradation mechanism study. This mini-review summarizes the latest research progress of the PFSCs' degradation studies. Based on the results achieved, one can identify the extrinsic and intrinsic stress factors that cause different degradation processes. Degradation pathways of the PFSCs at different positions in the cells will be discussed in detail, including the electrode, the buffer layer, and the photoactive layer. Special emphasis will be put on various degradation processes of the photoactive layers. In the meantime, the methods to suppress the degradation processes will be presented accordingly. This mini-review gives a comprehensive insight into the degradation mechanism and stability-improvement strategies of PFSCs, which has important guiding significance for the stability-improvement research of PSCs.

## 1. Introduction

With the advantages of lightweight, flexibility, translucency, and ease of large-area printing fabrication,<sup>[1–4]</sup> polymer solar cells (PSCs) are recognized as a promising green energy technology in the next future. PSCs have shown great application potentials in indoor microelectronics,<sup>[5]</sup> building integrated photovoltaic

Dr. L. Yan, Prof. C.-Q. Ma  
Printed Electronics Research Center  
Suzhou Institute of Nano-Tech and Nano-Bionics  
Chinese Academy of Sciences (CAS)  
Suzhou 215123, P. R. China  
E-mail: lpyan2014@sinano.ac.cn; cqma2011@sinano.ac.cn

Dr. L. Yan  
Institute of New Carbon Materials  
Taiyuan University of Technology  
79 Yingze Street, Taiyuan 030024, P. R. China

Dr. L. Yan  
Key Laboratory of Interface Science and Engineering in Advanced Materials  
Ministry of Education  
Taiyuan University of Technology  
Taiyuan 030024, P. R. China

The ORCID identification number(s) for the author(s) of this article can be found under <https://doi.org/10.1002/ente.202000920>.

DOI: 10.1002/ente.202000920

systems<sup>[6,7]</sup> and aerospace aircraft,<sup>[8]</sup> etc. PSCs have witnessed tremendous progress in the last decades, and the power conversion efficiency (PCE) has exceeded 18%, making the PSCs even more commercially relevant.<sup>[9,10]</sup> However, the operation lifetime of PSCs is still far away from sufficient for practical applications. Therefore, systematically exploring and understanding the degradation mechanism of PSCs and proposing effective methods to stabilize device performance are the most critical issues of PSCs.

In the history of PSCs, fullerene derivatives play an important role. Since the discovery of fullerene C<sub>60</sub> and C<sub>70</sub> (Figure 1) in the year 1985,<sup>[11]</sup> this new type of carbon allotrope received intensive research interest due to their unique physical and chemical properties. In 1995, Heeger and co-workers reported the first PSCs using C<sub>60</sub> and its derivatives [6,6]-phenyl-C<sub>61</sub>-butyric acid methyl ester (PC<sub>61</sub>BM) as the electron acceptor in blending with the polymer donor, poly(2-methoxy-5-(2'-ethylhexyloxy)-1,4-phenylene vinylene) (MEH-PPV).<sup>[12]</sup> Since then, conjugated polymer:fullerene blends are widely investigated, and various high-performance polymer donors and fullerene electron acceptors, such as poly(3-hexylthiophene) (P3HT),<sup>[13]</sup> poly(4,4-dialkyl-cyclopenta[2,1-*b*:3,4-*b'*]dithiophene-*alt*-2,1,3-benzothiadiazole) (PCPDTBT),<sup>[14]</sup> poly[(4,8-bis-(2-ethylhexyloxy)-benzo(1,2-*b*:4,5-*b'*)dithiophene)-2,6-diyl-*alt*-(4-(2-ethylhexyl)-3-fluorothieno[3,4-*b*]thiophene)-2-carboxylate-2,6-diyl)] (PTB7),<sup>[15]</sup> PM6,<sup>[16]</sup> [6,6]-phenyl-C<sub>71</sub>-butyric acid methyl ester (PC<sub>71</sub>BM),<sup>[17]</sup> [6,6] Diphenyl-C<sub>62</sub>-bis (butyric acid methyl ester) (Bis-PC<sub>61</sub>BM),<sup>[18]</sup> 1',1'',4',4''-tetrahydro-di[1,4]methanonaphthaleno[5,6]fullerene-C<sub>60</sub> (ICBA)<sup>[19]</sup> were developed (Figure 1), and high PCE of more than 10% were reported in these polymer:fullerene solar cells (PFSCs).<sup>[20]</sup> With the development of high-performance A–D–A type nonfullerene electron acceptor,<sup>[21–23]</sup> the PCE of polymer:non-fullerene solar cells (PNFSCs) exceeds that of fullerene-based cells in the year 2016. Even though fullerene derivatives are still used in ternary solar cells, such as PBDB-T:IT-M:bis-PC<sub>71</sub>BM,<sup>[24]</sup> PM6:2,2'-((2Z,2'Z)-((12,13-bis(2-ethylhexyl)-3,9-diundecyl-12,13-dihydro-[1,2,5]thiadiazolo[3,4-*e*]thieno[2'',3''':4',5']thieno[2',3':4,5]pyrrolo[3,2-*g*]thieno[2',3':4,5]thieno[3,2-*b*]indole-2,10-diyl)bis(methanylylidene))bis(5,6-difluoro-3-oxo-2,3-dihydro-1*H*-indene-2,1-diylidene))dimalononitrile (Y6):PC<sub>71</sub>BM,<sup>[25]</sup> PBDB-T-2F:Y6:PC<sub>71</sub>BM,<sup>[26]</sup> and tandem PSCs<sup>[27,28]</sup> due to their capability of morphology

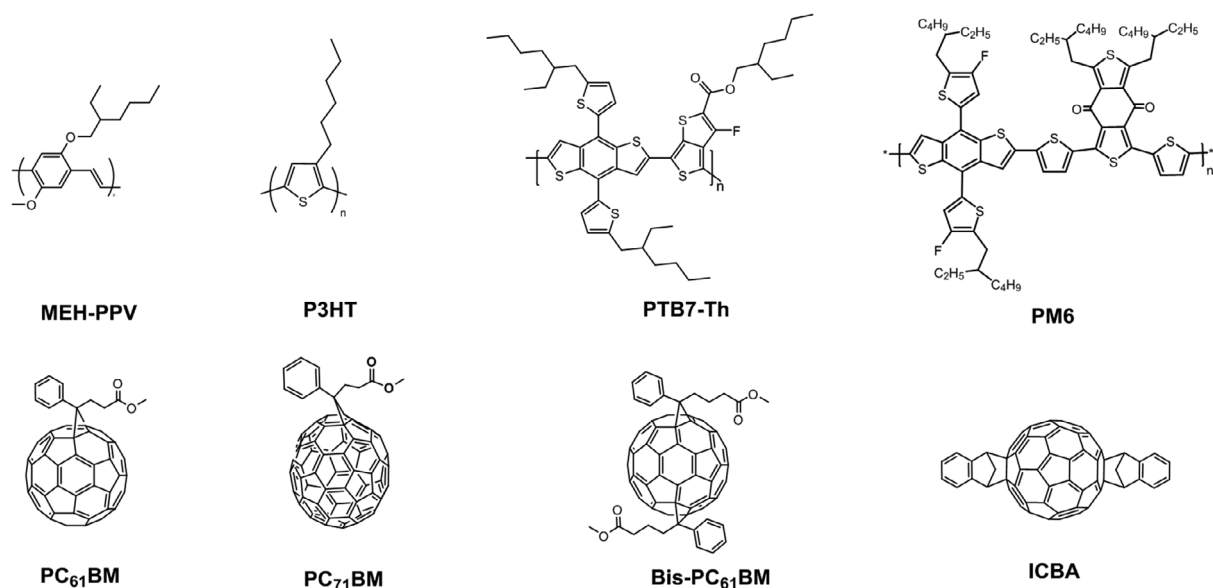


**Figure 1.** Chemical structure of some typical conjugated polymer donors and fullerene acceptors.

tuning and high open-circuit voltage ( $V_{OC}$ ) provided in the cell.

It should be pointed out that the fullerene derivatives not only play an irreplaceable role in the development of high-efficiency PSCs but also in understanding the working principle of PSCs. For example, using atomic force microscopy (AFM) and transmission electron microscopy (TEM) imaging of the polymer:fullerene blend film, scientists revealed the nanophase separation of the donor and acceptor within the blend films<sup>[29–31]</sup>; by quantitatively analyzing the influence of the fullerene lowest unoccupied molecular orbital (LUMO) energy on the  $V_{OC}$  of the final cell, Ohkita and co-workers confirmed that  $V_{OC}$  of the cell is directly related to the energy gap between the highest occupied molecular orbital (HOMO) of the donor and the LUMO of the acceptor<sup>[32]</sup>; by dissolving the fullerene crystalline domains with a high point good solvent-hexane, Yang and co-workers proved that high boiling point solvent additives can improve the nano phase separation within the blend films.<sup>[33]</sup> As the working principle of PFSCs is well understood, this type of solar cells is excellent model cells for the PSCs degradation mechanism studies. The stability study of PFSCs started even in the time when poly phenylenevinylene (PPV) was mainly used as the polymer donor. For example, Neugebauer et al. studied the photostability of poly (2-methoxy-5-(3',7'-dimethyloctyloxy)-1,4-phenylenevinylene (MDMO-PPV):PC<sub>61</sub>BM cells under light illumination and confirmed that photooxidation of PPV molecules is the main reason for the performance decay of the cells,<sup>[34]</sup> whereas Loos and co-workers reported the thermal stability of MDMO-PPV:PC<sub>61</sub>BM cells at the different annealing temperatures.<sup>[30,35]</sup> Since then, performance decay processes of PFSCs were widely investigated and various degradation mechanisms were clarified. In this review article, we first clarify the types of degradation processes according to the stress factors and then discuss various degradation pathways in detail according to the position of the degradation. Methods that can suppress the degradation process will be

included in the same section when discussing the degradation process, which should be able to help the readers to get a comprehensive overview of the different degradation behaviors of PSCs.

## 2. Degradation Processes of PFSCs

Many studies have demonstrated that degradation of PSCs results from the different degradation processes induced by various factors, including oxygen and water,<sup>[36–38]</sup> light irradiation,<sup>[39–41]</sup> thermal heating,<sup>[30,35]</sup> and electrical stresses.<sup>[42,43]</sup> Among these degradation processes, the decays of PSCs caused by water and/or oxygen in the atmosphere, in principle, can be suppressed by effective encapsulation (**Figure 2**). Therefore, the degradation process caused by water and/or oxygen can be considered as the extrinsic degradation process. Other degradation processes caused by light illumination, thermal heating, electrical stress, etc., can neither be avoided during PSCs' operation nor suppressed by encapsulation. Therefore, such decay processes are considered intrinsic degradation processes that depend on the stability of the materials and the device's layer structure. The only way to improve the intrinsic stability is to optimize the materials and device structure carefully. When the extrinsic degradation is eliminated by a perfect encapsulation, the materials and device structure of PSCs determine the maximum working life of the device, that is, the upper limit of the cell's lifetime. Knowing these, one can conclude that the intrinsic stability of the PSCs determines the upper limit of cells' lifetime, whereas extrinsic degradation processes will significantly lower the operation lifetime of PSCs than the upper lifetime limit. Understanding the degradation mechanism of PSCs and finding the proper method to suppress both degradation processes are essential for achieving a high operation lifetime of PSCs.

PSCs are usually multilayer structures and each functional layer has a thickness of around 10–100 hundred nanometers.<sup>[44]</sup>

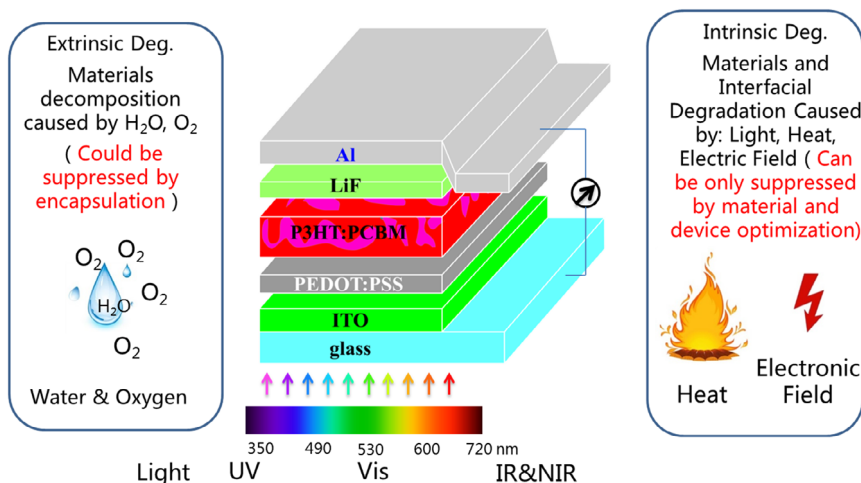


**Figure 2.** Various stress factors leading to the degradation of PSCs.

Such a nano-thin-film structure makes PSC more sensitive to the various stress factors than the traditional silicon or compound thin-film solar cells. Both intrinsic and extrinsic degradation processes can be found for the PSCs, and the degradation processes might happen on various positions, including the electrodes,<sup>[37,45]</sup> the interface layer,<sup>[46,47]</sup> and the photoactive layer.<sup>[48,49]</sup> In the following section, we will describe the well-known extrinsic and intrinsic degradation processes of the PSCs.

### 2.1. Extrinsic Degradation of PSC Caused by Water and Oxygen

If a PSC without encapsulation is operating in the atmosphere, the first problem concerning PSCs stability is the damage of materials by water and oxygen. When water and oxygen contact the cell directly, reactive reagents can penetrate into the PSCs through the pinholes of the metal electrode and/or the edges of the cells, causing the degradation of the electrode or the functional layer by the following-up chemical reaction.<sup>[36]</sup> The penetrated water and oxygen will oxidize the metal electrode forming a metal oxide interlayer between the electrode and photoactive layer,<sup>[37]</sup> which hinders the charge injection at the interface and causes an S-shaped  $J$ - $V$  curve of PSCs.<sup>[50]</sup> When water and oxygen reach the electrode buffer layer, such as poly(3,4-ethylenedioxythiophene)-poly(styrenesulfonate) (PEDOT:PSS),<sup>[51,52]</sup> MoO<sub>3</sub>,<sup>[53]</sup> ZnO,<sup>[54]</sup> LiF, and Ca,<sup>[55]</sup> both physical and chemical interactions of water and oxygen with these buffer layers will change the work function of the buffer layer and consequently decrease the device performance. Actually, diffusion of water and oxygen into the photoactive layer were also reported.<sup>[56]</sup> The chemical reaction of water and oxygen with conjugated organic semiconductor, especially under light illumination, dramatically causes the fast performance decay of the cells.<sup>[34,52,57]</sup> It should be pointed out that oxidization of fullerene molecules was also reported in PFSCs; even fullerene is a typically electron acceptor,<sup>[58]</sup> which would also cause the performance decay of solar cells through the creation of charge recombination sites within the photoactive layer. Interestingly, severe aggregation of fullerene molecules caused by water and oxygen was also

reported,<sup>[38]</sup> indicating that the influence of water and oxygen on the stability of PSCs can be complicated, and case study is highly needed for different type of cells.

As water and oxygen are external chemicals for the PSCs and direct contact is necessary to initiate PSCs decay, isolating water and oxygen from the cell with proper encapsulation can stop the decomposition process chain and suppress the undesired degradation of PSCs. As learned from the mature encapsulation technology for organic light-emitting diodes (OLED), many effective encapsulation materials have been used in PSCs, including organic<sup>[59–62]</sup> and organic–inorganic hybrid materials.<sup>[63,64]</sup> For example, Sapkota et al. reported that PSCs with a structure of Cr/Al/Cr/P3HT:PC<sub>61</sub>BM/PEDOT:PSS/metal-grid encapsulated with a nonpolar (pressure sensitive adhesive [PSA] with an unspecified barrier film) flexible barrier film can maintain 90% and 80% of their initial performance after aging for 12 000 h under continuous illumination at ambient air (50 °C and 6% RH).<sup>[59]</sup> Romero-Gomez et al. incorporated a dielectric multilayer stack of MgF<sub>2</sub>/MoO<sub>3</sub> (550 nm) to semitransparent PTB7-PC<sub>71</sub>BM solar cell and ultimately increased the shelf lifetime close to ten times.<sup>[60]</sup> Tsai and Chang utilized atomic layer deposition (ALD) to deposit a 26 nm ALD Al<sub>2</sub>O<sub>3</sub>/HfO<sub>2</sub> composite layer, which showed a low water-vapor transmission rate of (WVTR)  $<5 \times 10^{-4} \text{ g m}^{-2} \text{ day}^{-1}$ . The composite layer effectively isolates water and oxygen from the cell, and the P3HT:PC<sub>61</sub>BM solar cells maintained >70% of their initial PCE upon >1800 h in a 65 °C/60% RH.<sup>[62]</sup> Gleason and co-workers reported the use of a composite layer consisting poly(divinylbenzene) (PDVB) and a CeO<sub>2</sub> UV-screening layer to encapsulate the PSCs, which effectively improve the stability ( $\approx 5$ -fold increase on the half-life) of PSCs (40 °C, in the air).<sup>[64]</sup> **Table 1** summarizes the stability of some typical encapsulated PFSCs. It can be seen that the commonly used encapsulating materials for PFSCs are organic, inorganic, and organic–inorganic hybrid materials, and a good encapsulation can successfully suppress the PSCs' extrinsic degradation processes. However, as encapsulation cost is still high, the development of highly stable conjugated organic semiconductors and reducing the encapsulation cost are still highly needed for the PSC community.

**Table 1.** Summary of the stability of typical encapsulated PFSCs and unencapsulated PNFSCs.

PSCs types	Active area	Device structure	PCE [%]	Encapsulation materials	Aging condition	Life time <sup>a)</sup>	Ref.
Rigid PFSCs	Small area	ITO/PEDOT:PSS/P3HT: PC <sub>61</sub> BM/Al	3.62	Al <sub>2</sub> O <sub>3</sub> /HfO <sub>2</sub> nanolaminated film overcoated with an epoxy resin protection layer	In ambient light at 28 °C and 60% relative humidity	T <sub>50</sub> => 600 h	[196]
	Small area	ITO/ZnO/P3HT: PC <sub>61</sub> BM/PEDOT: PSS + PTE/Al	2.83	UV resin (400 nm) encapsulation with ZnO buffer layer	In air	The PCE degrades by 20.5% after 672 h.	[197]
	0.12 cm <sup>2</sup>	ITO/ZnO/P3HT: PC <sub>61</sub> BM/PEDOT: PSS/Ag	2.78	poly(perfluorodecylmethacrylate) (PFDMA)	In an air ambient	Reduction of 23.3% after 456 h of air exposure	[198]
	0.16 cm <sup>2</sup>	ITO/PEDOT:PSS/P3HT: PC <sub>61</sub> BM/Al	2.9	Ulathrin AlO <sub>x</sub>	In ambient air, under constant indoor illumination.	Retained 30% efficiency after 2000 h of air exposure	[199]
	Small area	ITO/ZnO/PEIE/PTB7: PC <sub>70</sub> BM/MoO <sub>3</sub> /Ag	7.53	SiNx/SiOx barrier film	In ambient air (relative humidity: 40–60%; temperature: about 25 °C)	Remained above 86% of the initial value even after 2000 h of storage in air	[200]
	0.1 cm <sup>2</sup>	ITO/ZnO/P3HT: PC <sub>61</sub> BM/PEDOT: PSS/Ag	2.96	Deposition of a perhydropolysilazane (PHPS) ink and its subsequent conversion into a silica layer by deep UV irradiation	Under continuous irradiation in ambient air in the chamber of a sun simulator.	Lose around 29% of the initial performance within 350 h.	[201]
	0.078 cm <sup>2</sup>	ITO/ZnO/PEIE/P3HT: PC <sub>61</sub> BM/MoO <sub>3</sub> /Ag	4.16	Reduced graphene oxide (rGO)/PEN films	Temperature of 25 ± 5 °C and RH of 100%.	Maintains photovoltaic performance as high as 88% of the initial efficiency after 28 days.	[202]
Flexible PFSCs	0.28 cm <sup>2</sup>	ITO/ZnO/P3HT: PC <sub>61</sub> BM/PEDOT: PSS/Ag	2.5	PET/Inorganic layer/PVA/inorganic layer, inorganic layer prepared from PHPS	In an ambient atmosphere at 35 °C under AM 1.5 illumination of about 1000 W m <sup>-2</sup> .	Reduce the power loss over 450 h to less than 10%	[203]
	186 cm <sup>2</sup>	Ag grid electrode/PEDOT:PSS/ZnO/P3HT: PC <sub>61</sub> BM/PEDOT: PSS/Ag	1.62	Encapsulated between two sheets of Amcor barrier foil using a UV curable adhesive from DELO.	–	ISOS-D-1, T <sub>80</sub> = 2800 h ISOS-D-2, T <sub>80</sub> = 5000 h; ISOS-LL, T <sub>80</sub> = 5000 h; ISOS-L-2, T <sub>80</sub> = 5000 h; ISOS-O, T <sub>80</sub> = 5000 h;	[204]
	17.1 cm <sup>2</sup>	ITO/PEDOT:PSS/MDMO-PPV: PC <sub>61</sub> BM/Al	0.035	PEN + Super barrier (alternating transparent layers of SiOx and PECVD deposited organosilicon).	In the dark, under ambient air (20–25 °C; 35–50% relative humidity)	T <sub>54</sub> = 3000 h	[205]
	70-100 cm <sup>2</sup>	Ag grid/PEDOT: PSS/ZnO/P3HT: PC <sub>61</sub> BM/PEDOT: PSS/Ag grid	0.86	Laminating the modules between two PET sheets (125 μm) of the barrier foil with the use of a UV curable adhesive	ISOS-O	Maintained 95% of the initial performance after 1 year of outdoor testing	[206]
	50 cm <sup>2</sup>	PET/ITO/ZnO/P3HT: PC <sub>61</sub> BM/PEDOT:PSS/Ag	0.84	Consists of 3 m Ultra barrier solar film barrier encapsulant layers laminated onto the front and back faces of the printed module, together with an edge-sealing tape to provide additional moisture barrier.	Outdoor exposure at CSIRO's site in Clayton, Victoria (37.91° S, 145.14° E)	A shelf-life of more than 5 years, and no evidence of degradation after 13 months' exposure under outdoor conditions	[207]
Rigid PNFSCs	0.04 cm <sup>2</sup>	ITO/ZnO/PT2:EH-INIC3/POE/Ag	13.47	Unencapsulated devices	Storage in air, humidity = 40%	After storage in air after 2350 h, solar cell still remained 91.2% of initial PCE values.	[66]
	Small area	ITO/ZnO/PBDB-T: ITIC-2F/MoOx/Al	8	–	Under N <sub>2</sub> without moisture, an array of white LEDs was used as light source (without UV) with intensity equivalent to 1 sun	Promising extrapolated operational lifetime approaching 10 years	[67]

<sup>a)</sup>Time that reaches α% of its initial PCE.

Studies have shown that PSCs using nonfullerenes instead of fullerene as acceptors show better stability than PFSCs.<sup>[65]</sup> Although there are few studies on the air stability of PNFSCs at present,<sup>[66]</sup> studies showed that PNFSCs in an inert atmosphere exhibit extremely long working stability, and the device life were predicted to be 10 years.<sup>[67]</sup> In addition, people are also exploring the use of additives to improve the stability of PSCs. As the reactive oxygen radicals formed under light illumination in the ambient atmosphere, the use of reactive oxygen or radical scavenger was also reported to improve the stability of the polymer:fullerene cells. For example, Turkovic et al. reported the use of a hindered phenol, Arenox A76, as the additive in the P3HT:PC<sub>61</sub>BM cells, which effectively reduce the radicals within the photoactive layer and a three times increase in the accumulated power generation (APG) was measured for the cell with the phenol stabilizer.<sup>[68]</sup> After that, they doped a hydroperoxide decomposer (Advapak NEO-1120) into photoactive layer, which effectively decrease the formed free radicals emerging from homolytic split of hydroperoxides, and ultimately improve the device stability.<sup>[69]</sup> Moreover, they use the UV absorber 2(4,6-diphenyl-1,3,5-triazin-2-yl)5[(hexyl)oxy]phenol as the stabilizing additive, which also reduces the free radicals in photoactive layer, resulting in improved device stability.<sup>[70]</sup> Following this, the same research group introduced a small molecule  $\beta$ -carotene as a free-radical quencher to PTB7:PC<sub>71</sub>BM and P3HT:PC<sub>61</sub>BM solar cells, which can also effectively improve the efficiency and stability of the device.<sup>[71]</sup> In short summary, by knowing the chemical degradation mechanism, one should be able to find a proper additive to suppress the degradation process.

## 2.2. Intrinsic Degradation of PFSCs

In contrast to PSCs' extrinsic degradation, the intrinsic degradation processes are induced by those unavoidable factors such as light irradiation, thermal heating, or electric field when the cell is under operation.<sup>[48]</sup> As mentioned earlier, such degradation processes can not be suppressed by external encapsulation, and the stability of PSCs can only be improved by materials and device structure optimization. Therefore, understanding PSCs' intrinsic degradation mechanism could give important guidelines for the synthesis of highly stable materials and the optimization of the device structure.

As light illumination is the most essential step for a solar cell, light-induced degradations of PSCs have to be investigated very carefully. Unlike in inorganic semiconductor-based solar cells, where light illumination generates free chargers within the semiconductors layer, light absorption by a PSC generates high-energy excitons within the photoactive layer, where the electron-hole pairs are bonded together by the Coulomb attraction.<sup>[72,73]</sup> The relative long lifetime and energy of excitons could induce the following up chemical reaction of the organic molecules, that could lead to the decomposition of the photoactive layer.<sup>[42,74,75]</sup> More severely, photooxidation of the organic compounds would happen when oxygen or water molecules are diffused into the photoactive layer, which will dramatically increase the photon bleaching of the photoactive layer, and decrease the lifetime of the cells. Interestingly, McGehee and co-workers<sup>[76]</sup> and Li and co-workers<sup>[77-79]</sup> proved that fullerene

molecules are able to slow down the photooxidation of the organic semiconductors, and this could be a useful way in improving the stability of PSCs. Nevertheless, as discussed earlier, such a photooxidation of the organic compounds by water and oxygen using proper encapsulation.

In a bulk heterojunction solar cell, nano phase separation of the donor and acceptor determines the charge generation and separation rate.<sup>[80,81]</sup> Therefore, a stabilized nanomorphology is necessary to achieve a stable PSC. The bicontinuous phase morphology of photoactive layer of PSCs is reported to be formed through spinodal demixing and subsequent crystallization of the donor and acceptor.<sup>[82]</sup> Moreover, the fraction of higher ordered polymer domains is affected by the fullerene distribution over the film thickness as well as the substrate and air interface, especially for the heated films.<sup>[83]</sup> Moreover, organic polymers are typically not fully crystallized materials and molecular motion can never stop at operation temperature, nanomorphology changes of the photoactive layer is theoretically unavoidable. Knowing that molecular motion is dependent on the temperature, therefore nanomorphology changes induced by thermal heating is the second important intrinsic degradation pathways for PSCs.<sup>[84,85]</sup> When fullerene acceptors is blended with an amorphous polymer, that crystallization of fullerene molecules happens when the polymer blend was heated.<sup>[30,35]</sup> However, when fullerene acceptor is blended with a semicrystalline polymer, such as P3HT, due to the crystallization of polymer, thermal-induced morphology changes of the polymer blend turns to be complicated.<sup>[71]</sup> Therefore, thermal stability of the PSCs is also highly dependent on the nature of organic materials in the cells.

Last but not the least is the electric-field-induced degradation of the PSCs. Although electric-field-induced degradations of perovskite solar cells were reported in the literature,<sup>[86,87]</sup> and degradation behaviors of perovskite solar cells under different bias are suggested to be the standard for the stability test,<sup>[88]</sup> there is no direct reported on the electric-field-induced degradation of PSCs. Recently, both Brabec and our research groups found that PSCs exhibit an external-load-dependent degradation behavior.<sup>[42,75]</sup> It is therefore expectable that electric field could also induce the degradation of PSCs.

## 3. Various Degradation Pathways of the PFSCs

### 3.1. Degradation of the Top Metal Electrode

The most widely used metal electrode for PSCs are silver (Ag) and aluminum (Al). It is known that thin Al film can be oxidized by water and oxygen due to its low work function (4.0–4.3 eV).<sup>[89-91]</sup> Therefore, corrosion of the Al electrode is one of the main reasons that cause the extrinsic degradation of PSCs.<sup>[92]</sup> Ag has a higher work function (4.7 eV) than Al.<sup>[93]</sup> Therefore, Ag electrode should be more stable than Al electrode in against water and oxygen.<sup>[94]</sup> On the other hand, the high work function of the Ag electrode makes it more suitable for hole injection than electrode injection. Therefore, Ag electrode is usually used in structure inverted PSCs as the anode.<sup>[28,95]</sup> However, by inserting an interfacial modification layer of polyethylenimine (PEI) (or polyethylenimine ethoxylated [PEIE]), the work function of Ag

electrode can be reduced to 3.6–3.7 eV,<sup>[96]</sup> making Ag electrode suitable for use as the cathode in PSCs as well. Nevertheless, using proper encapsulation, the chemical corrosion of the top electrode can be suppressed, and the stability of the cell can be significantly improved.<sup>[97]</sup>

However, even in an environment without water and oxygen, electrodes of PSCs might decay slowly under light illumination and/or electric field stress, which leads to the performance decay of the PSCs. The first pathway for the top electrode decay is the migration of metal atoms during operation. Hoppe and co-workers reported that the Ag atoms could penetrate through the PEDOT:PSS and the photoactive layer driven by electromigration at the electric field (**Figure 3**), leading to shunts within the cell.<sup>[92]</sup> Also, for the cells with Al electrode, metal penetration was also reported, which leads to the fast performance decay of the cells.<sup>[92]</sup> Such metal atoms migrations, on the one hand, change the energy levels of the buffer layer and thus affect the charge extraction and transfer processes, on the other hand, will form traps in the photoactive layer and create significant charge recombination.

As the change of metal electrode's work function and the migration of metal atoms are not avoidable, the long-term stability of PSCs using a metal electrode could be a problem. Therefore, searching for electric-field insensitive top electrode is still highly needed for PSCs. Recently, carbon electrodes have been reported in perovskite solar cells to improve device stability.<sup>[98,99]</sup> Due to its excellent chemical and physical stability, carbon electrode could also be good for use in PSCs.<sup>[100]</sup> However, due to the low conductivity of carbon electrodes and the poor interfacial connection between the buffer layer and the carbon electrode, the performance of this type of cell is still lower than the metal electrode-based cells.

### 3.2. Degradation of the Electrode Buffer Layer

The electrode buffer layer that is inerted between the electrode and the photoactive layer displays multiple functions in PSCs, including charge selection at the interface, adjusting the electronic band alignment within the cell, and isolating the metal electrode from the photoactive layer. Measuring the change in the buffer layer during aging is quite challenging as the buffer layer is typically under the opaque metal electrode.

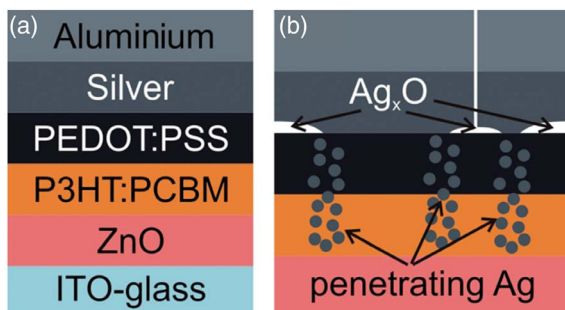


**Figure 3.** Ag electrode penetrates through the PEDOT:PSS into the photoactive layer, causing shunts of PSCs. Adapted with permission.<sup>[92]</sup> Copyright 2012, The Royal Society of Chemistry.

Experimentally, one can remove the top electrode and the buffer layer of the aged cell and then redeposit a new buffer layer and the top electrode. If the cell with refreshed buffer layer and top electrode showed performance recovery, one can confirm that decay of the buffer layer is the main reason for the solar cell performance decay.<sup>[46,47,101,102]</sup> With this method, many interfacial layer decays were clearly clarified, including the interfacial diffusion,<sup>[47]</sup> and the interfacial chemical reaction.<sup>[101,102]</sup>

#### 3.2.1. Cathode Buffer Layer

According to the interlayer's charge-transporting capability, the buffer layer can be classified as cathode buffer layer and anode buffer layer, which facilitates electron and hole transporting. LiF is the most widely used electron buffer layer material for the aluminum electrode in conventional PSCs.<sup>[103,104]</sup> The insertion of LiF layer can simultaneously increase the  $V_{OC}$  and FF of the cell.<sup>[103,105]</sup> However, LiF was reported to be easily dissociated and the  $Li^+$  can diffuse into the photoactive layer,<sup>[106–108]</sup> especially when the cell is heated, causing a serious performance decay of PSCs. Lee and Jeon studied the aging behavior of PSCs with the structure of ITO/PEDOT:PSS/P3HT:PC<sub>61</sub>BM/LiF/Al.<sup>[106]</sup> They found that LiF is dissociated into  $Li^+$  and  $F^-$  during deposition of Al and the produced  $Li^+$  will diffuse into the photoactive layer during lifetime test (**Figure 4a**), which cause significant reduction in  $V_{OC}$ ,  $J_{SC}$ , and PCE of PSCs. With the same device structure of PSCs, Chen and co-workers also found that preannealing will cause LiF diffuse into the P3HT:PC<sub>61</sub>BM active layers of PSCs, which decrease the crystallinity of P3HT and ultimately lead to a decline of device performance.<sup>[107]</sup> Our previous research also proved that when the LiF-based P3HT:PC<sub>61</sub>BM solar cells are heated at 80°, its device performance will decay to 80% of the initial performance within 42 h.<sup>[108]</sup> Other more stable cathode buffer materials were then developed for PSCs, including metal oxide<sup>[109,110]</sup> and carbon materials.<sup>[108,111,112]</sup>

ZnO is the most efficient electronic buffer layer used in inverted PSCs due to the advantages of ease of synthesis, good electron mobility as well as good solution processability.<sup>[113,114]</sup> ZnO is even used in roll-to-roll printed large-area cells.<sup>[115]</sup> Unlike LiF, atoms in ZnO is more strongly bonded. Therefore, ZnO-based PSCs showed a greatly improved thermal stability than the LiF-based cell.<sup>[116]</sup> However, the solution-processed ZnO layer usually contains many defects, such as dangling bonds,<sup>[117]</sup> adsorbed oxygen.<sup>[118,119]</sup> PSCs based on the ZnO layer usually exhibit an S-shaped  $J-V$  curve yielding poor device performance. Such an unsatisfied interfacial charge injection and transportation can be improved by UV irradiation, which was attributed to the release of absorbed oxygen under UV illumination. As absorption and deabsorption of oxygen is reversible, our results revealed that the S-shaped  $J-V$  curves will appear after the solar cells are stored in the dark for a period of time.<sup>[120]</sup> Moreover, Wu and co-workers found that excessive UV irradiation of ZnO-based PSCs can cause the  $V_{OC}$  of PSCs with a device structure of ITO/ZnO/P3HT:PC<sub>61</sub>BM/MoO<sub>3</sub>/Ag to decay rapidly.<sup>[121]</sup> They associated the decay of PSCs to the continuous UV irradiation that reduced the hole-blocking ability of ZnO. Similarly, Katz and co-workers found that the

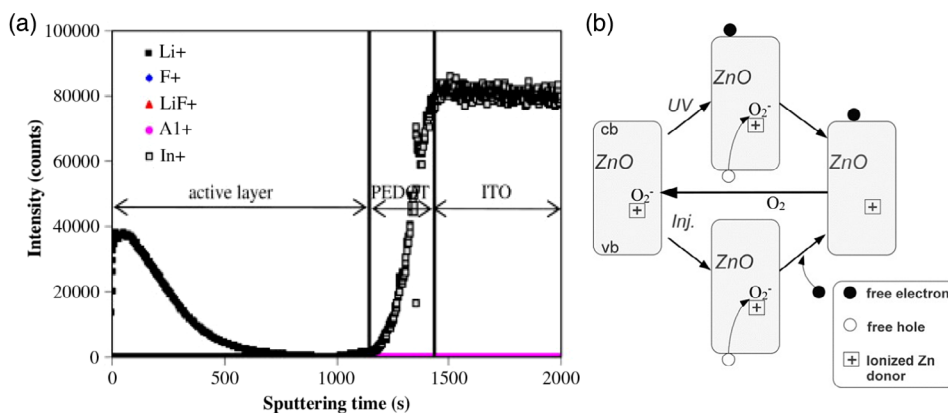


**Figure 4.** a)  $\text{Li}^+$  penetrates into the photoactive layer, causing a serious performance decay of PSCs. Adapted with permission.<sup>[106]</sup> Copyright 2012, Elsevier B.V. b) Continuous UV irradiation reduces the hole-blocking ability of ZnO. Reproduced with permission.<sup>[43]</sup> Copyright 2019, WILEY-VCH.

concentrated sunlight irradiation will lead generation of shunts in the ZnO hole-blocking layer of PSCs with a device structure of ITO/ZnO/P3HT:PC<sub>61</sub>BM/PEDOT:PSS/Ag (Figure 4b). Interestingly, they reported that such shunts within the ZnO layer could be prevented by electrical treatment (short pulses of the reverse bias).<sup>[43]</sup> Olson and co-workers investigated the stability of PSCs with a device structure of ITO/ZnO/P3HT:ICBA/MoO<sub>3</sub>/Ag based on ZnO prepared from different precursors (zinc acetate (ZnAc) and diethylzinc (deZn)) and found that the presence of Zn defects on the surface of ZnO would affect the device stability.<sup>[122]</sup> In addition to ZnO, SnO<sub>2</sub> was also used as the cathode buffer layer in PSCs showing improved stability.<sup>[95]</sup> Other than these metal oxide, Tan and co-workers used titanium (diisopropoxide)-bis-(2,4-pentanedionate) (TIPD) as an electron buffer layer of PBDTBD:ITIC-M solar cells, which was found to be able to tune the vertical phase separation of the photoactive layer, and simultaneously improve the efficiency and stability of the cell.<sup>[123]</sup>

As surface defects of ZnO are the main reason causing the performance decay of the PSCs, using organic ligands to passivate the surface defects is proposed to be an effective way to improve the stability of the PSCs having ZnO buffer layer.<sup>[124,125]</sup> For example, Xiao and co-workers reported that doping bis (tri-fluoromethane)sulfonimide lithium salt (Li-TFSI) into ZnO film can increase the electrical conductivity and charge-extraction ability of ZnO and also can improve the device stability of PSCs consisting of ITO/PEDOT:PSS/poly[4,8-bis(5-(2-ethylhexyl)thiophen-2-yl)benzo[1,2-b;4,5-b']dithiophene-2,6-diyl-alt-(4-(2-ethylhexyl)-3-fluorothiopheno[3,4-b]thiophene)-2-carboxylate-2,6-diyl] (PTB7-Th):PC<sub>71</sub>BM/ZnO + Li-TFSI/Al.<sup>[124]</sup> We recently proved that using a nanocomposite of ZnO together with poly [(9,9-bis(3'-(N,N-dimethylamino)propyl)-2,7-fluorene)-alt-2,7-(9,9-dioctyl)-fluorene] (PFN) as ETL of PSCs can simultaneously improve the efficiency and stability of PSCs (Figure 5a).<sup>[126]</sup> Moreover, we synthesized a 3-aminopropyltrimethoxysilane (APTMS)-capped ZnO (ZnO@APTMS) nanoparticles and utilized them as ETL of inverted PSCs (Figure 5b). The capping of ZnO with APTMS not only suppressed the

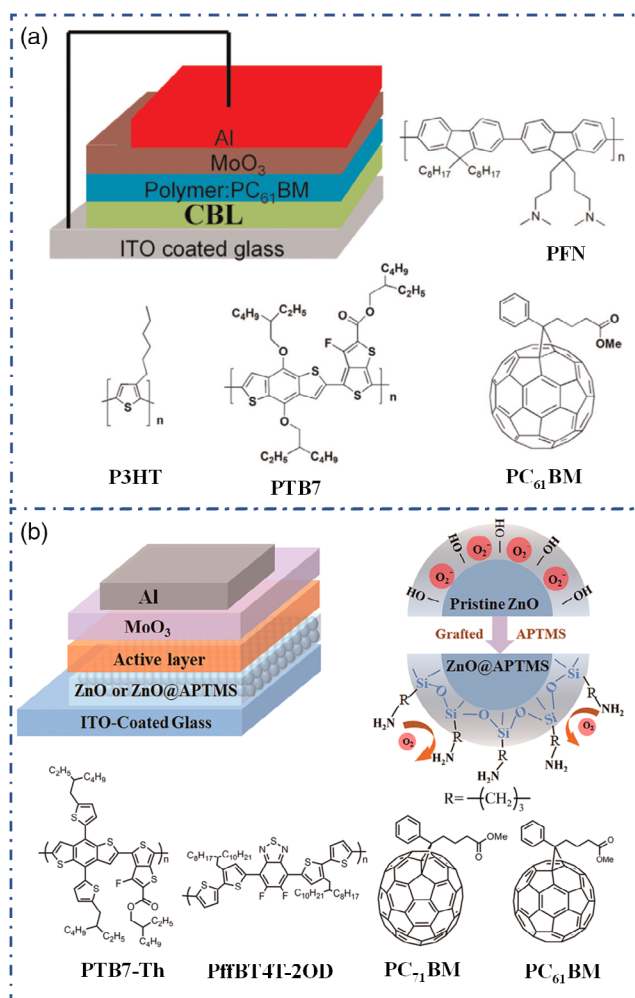


**Figure 5.** a) PFN:ZnO nanocomposite. Adapted with permission.<sup>[105]</sup> Copyright 2015, Elsevier B.V. b) ZnO@APTMS nanoparticle serve as the electron-transfer layer of PSCs. Adapted with permission.<sup>[125]</sup> Copyright 2018, American Chemical Society.

light-soaking effect but also improved the stability of devices.<sup>[125]</sup> Interestingly, such surface-decorated ZnO nanoparticles are found to be able to improve the long-term and thermal stability of perovskite solar cells as well, clearly demonstrating the concept of developing highly stable metal oxide for use in new-generation thin-film solar cells.<sup>[127]</sup>

In addition to metal oxide, carbon quantum dots (CQDs) are also found to be a good cathode materials for use in PSCs. For example, we recently replaced LiF with high-crystallinity carbon quantum dots (C-CQDs) as the electron-transport layer of conventional PSCs (**Figure 6**). Finally, C-CQDs-based devices achieve performance comparable to LiF devices, and the thermal stability has been greatly improved. The  $T_{80}$  of C-CQDs-based solar cell was more three times longer than that of LiF-based devices.<sup>[108]</sup> It is worth pointed that, during the experiment, we found that the PSCs only treated with methanol (solvent of C-CQDs) without inserting the electron-transport layer also showed higher thermal stability, but their device performance is far worse than C-CQDs and LiF-based devices. In addition, we utilized N,S-doped carbon quantum dots (N,S-CQDs) to dop ZnO and used the ZnO:N,S-CQDs as the electron-transport layer of inverted PSCs consisting of ITO/ZnO:N,S-CQDs/PTB7-Th:PC<sub>71</sub>BM/MoO<sub>3</sub>/Al. The doping of N,S-CQDs successfully passivated the surface defects of ZnO, which successfully eliminated the light-soaking effect of device.<sup>[128]</sup> Furthermore, we used CQDs to induce the growth of ZnO crystals and successfully synthesized ZnO-coated CQDs (CQDs@ZnO) nanoparticles, which suppressed defects of ZnO and improved device performance of CQDs@ZnO-based solar cells consisting of ITO/CQDs@ZnO/PM6:IT-4F /MoO<sub>3</sub>/Al.<sup>[129]</sup>

### 3.2.2. Anode Buffer Layer

Poly(3,4-ethylenedioxythiophene):poly(styrenesulfonate) (PEDOT:PSS) is a common hole-transport layer for PSCs,<sup>[130,131]</sup> even though PEDOT:PSS has quite a few drawbacks that affect the stability of PSCs. PEDOT:PSS is a highly acidic mixture with a pH of 1–3. Such an acidic nature would corrode the ITO electrode yielding In<sup>3+</sup> ions that can easily diffuse into the photoactive layer and cause performance decay.<sup>[132]</sup> Norrman et al. reported that PSS will undergo phase separation and even diffuse into the C12-PSV/C60 photoactive layer and react with C12-PSV.<sup>[133]</sup> Vitoratos et al. reported that the conductivity of PEDOT:PSS will decrease with increasing temperature.<sup>[134]</sup> They attributed the thermal instability of the PEDOT:PSS layer to the conformation changes.

MoO<sub>3</sub> is widely used as the hole-transport layer in inverted PSCs due to its high work function, high hydrophobicity, and good oxidation resistance.<sup>[135,136]</sup> Numerous research works reported that MoO<sub>3</sub> can serve as an interface layer to effectively improve PSCs' stability.<sup>[55,60,137]</sup> However, there are also reports revealing that MoO<sub>3</sub> may cause the degradation of the PSCs when the cell is under continuous light illumination. Chambon and co-workers found that MoO<sub>3</sub> reacts with Ag electrodes under heating, resulting in  $V_{OC}$  decay of PSCs.<sup>[138]</sup> Such degradation process can be suppressed by replacing Ag with Al. Hany and co-workers reported that Mo<sup>5+</sup> is formed in MoO<sub>3</sub> layer during illumination, which decrease the work fuction of MoO<sub>3</sub> and result in an unfavorable change in the energy alignment, resulting in the performance decay of PSCs.<sup>[139]</sup> Our recent work found that the proportion of Mo<sup>5+</sup> in MoO<sub>3</sub> will

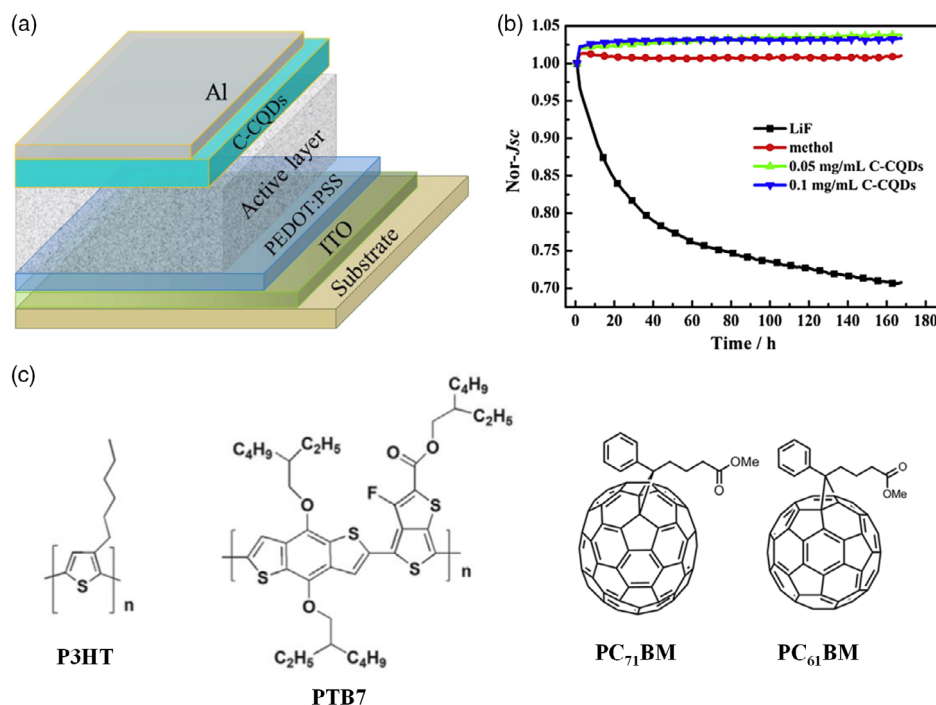


**Figure 6.** a) CQD replaces LiF as the electron-transport layer of standard structure PSCs, greatly improving; b) the thermal stability of the device; c) the molecular structures of P3HT, PTB7, PC<sub>71</sub>BM, and PC<sub>61</sub>BM. Adapted with permission.<sup>[108]</sup> Copyright 2016, Elsevier B.V.

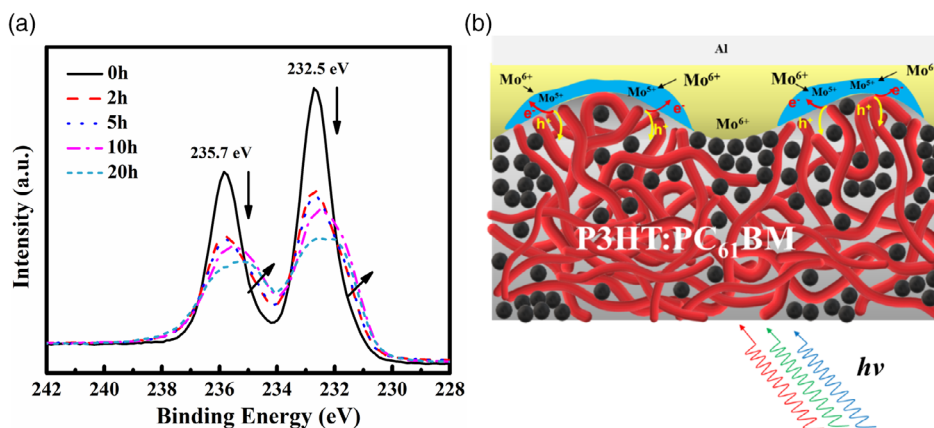


**Figure 7.** a) The proportion of  $\text{Mo}^{5+}$  in P3HT/ $\text{MoO}_3$  films increases with the prolonged illumination time. b) Schematic diagram of interfacial photochemical reduction of  $\text{MoO}_3$  by P3HT that causes decay of the cell. Adapted with permission.<sup>[102]</sup> Copyright 2020, American Chemical Society.

increase with the extension of the illumination time.<sup>[101,102]</sup> Subsequent comparative experiments proved that  $\text{MoO}_3$  and P3HT undergo a light-induced reduction reaction, and part of  $\text{Mo}^{6+}$  in  $\text{MoO}_3$  is reduced by P3HT to  $\text{Mo}^{5+}$ , which causes charge recombination at the interface and ultimately lead to the decay of  $V_{\text{OC}}$  and FF of P3HT: $\text{PC}_{61}\text{BM}$  PSCs.<sup>[102]</sup> Moreover, we further confirmed that the light-induced reduction reaction mainly occurs at the P3HT/ $\text{MoO}_3$  interface.<sup>[101]</sup> The light-induced reduction reaction decrease the work function of  $\text{MoO}_3$ , thereby weakening the dipole at the P3HT/ $\text{MoO}_3$  interface, and ultimately affecting the charge transport over time (Figure 7). Therefore, we designed to insert a layer of C60 (1.5–3 nm) between the photoactive layer and  $\text{MoO}_3$  to isolate the contact between  $\text{MoO}_3$  and P3HT, and finally effectively improve the stability of P3HT:bis- $\text{PC}_{61}\text{BM}$  solar cells.<sup>[101]</sup> In addition, the mentioned issues of  $\text{MoO}_3$ -induced degradation of PSCs can also be alleviated by a change in deposition technique. Ahmadpour et al. recently used reactive sputtering instead of thermal evaporation to deposit  $\text{MoO}_3$  film, which enables more precise tuning of  $\text{MoO}_3$  properties.<sup>[140]</sup> It has been shown that the stability of PSCs can be significantly raised (as compared with the standard thermally evaporated  $\text{MoO}_3$ ) using superoxidized  $\text{MoO}_{3.2}$  films grown by reactive sputtering and recrystallized at elevated temperatures.

### 3.3. Degradation of the Photoactive Layer

#### 3.3.1. Triplet Excitons Related Fullerene Dimerization

For fullerene-based PSCs, especially for  $\text{PC}_{61}\text{BM}$ -based solar cell, the most critical factor affecting their lifetime is the dimerization

of fullerene molecules. Fullerene  $\text{C}_{60}$  molecules were reported to undergo a [2 + 2] cycloaddition reactions to form dimers even in an inert atmosphere or vacuum,<sup>[141–143]</sup> and this process is reversible at high temperature ( $T > 100^\circ\text{C}$ ).<sup>[144]</sup> Similarly,  $\text{PC}_{61}\text{BM}$  also undergoes dimerization during illumination (Figure 8),<sup>[145]</sup> which causes the short circuit ( $J_{\text{SC}}$ ) of PSCs to decline by 20–50% in a short time.<sup>[48,146]</sup> The typical feature of  $\text{PC}_{61}\text{BM}$  dimer formation in the aged PSCs is that the increased absorption band at 320 nm (Figure 9c), while the EQE response at 350–450 nm is weakened.<sup>[42,74]</sup> In addition,  $\text{PC}_{61}\text{BM}$  dimer can also be detected by high-performance liquid chromatography (HPLC) (Figure 9d),<sup>[42,74]</sup> Raman, and FTIR spectroscopy.<sup>[147,148]</sup>

The formation of fullerene dimers causing the  $J_{\text{SC}}$  decay of PSCs is ascribed to two different ways: one is that the formation of  $\text{PC}_{61}\text{BM}$  dimers affects the charge separation at the interface of donor and acceptor, and the other one is that  $\text{PC}_{61}\text{BM}$  dimers act as exciton traps in the photoactive layer. McGehee and co-workers systematically investigated the dimerization of  $\text{PC}_{61}\text{BM}$  and found that the nanomorphology of the photoactive layer and the electrical bias significantly affected the dimerization reaction.<sup>[42]</sup> Our previous research work also found that P3HT: $\text{PC}_{61}\text{BM}$  solar cells exhibit significant external load-dependent decay behavior. That is, the cell's decay rate is directly related to the external load attached to the cell during aging (Figure 10a).<sup>[75]</sup> This is because the external load will affect the concentration of excitons in the solar cell and a high concentration of excitons will accelerate the dimerization of  $\text{PC}_{61}\text{BM}$  (Figure 10b). Such an exciton concentration-dependent degradation process implies that the dimerization process is triplet excitons related (Figure 11).<sup>[42,149]</sup>

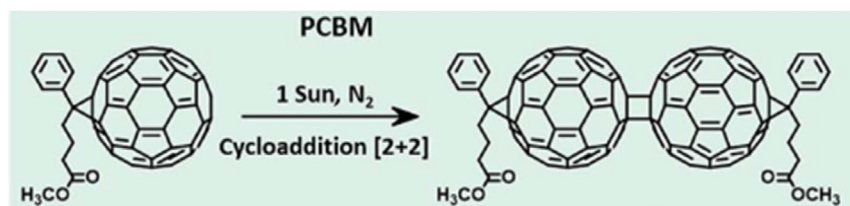


**Figure 8.** Dimerization of  $\text{PC}_{61}\text{BM}$ . Adapted with permission.<sup>[145]</sup> Copyright 2017, Royal Society of Chemistry.

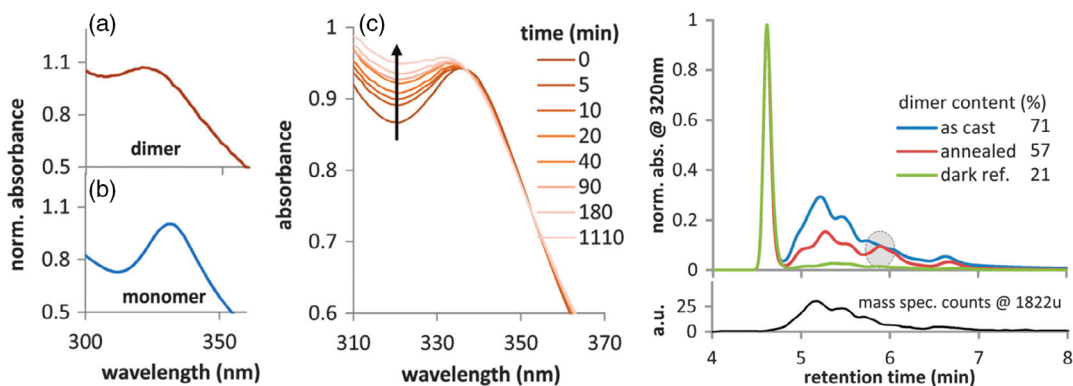


**Figure 9.** HPLC spectra of PC<sub>61</sub>BM dimer under illumination and redissolved (left). UV-vis absorption changes of the PC<sub>61</sub>BM films under light illumination (right). Adapted with permission.<sup>[42]</sup> Copyright 2016, Royal Society of Chemistry.

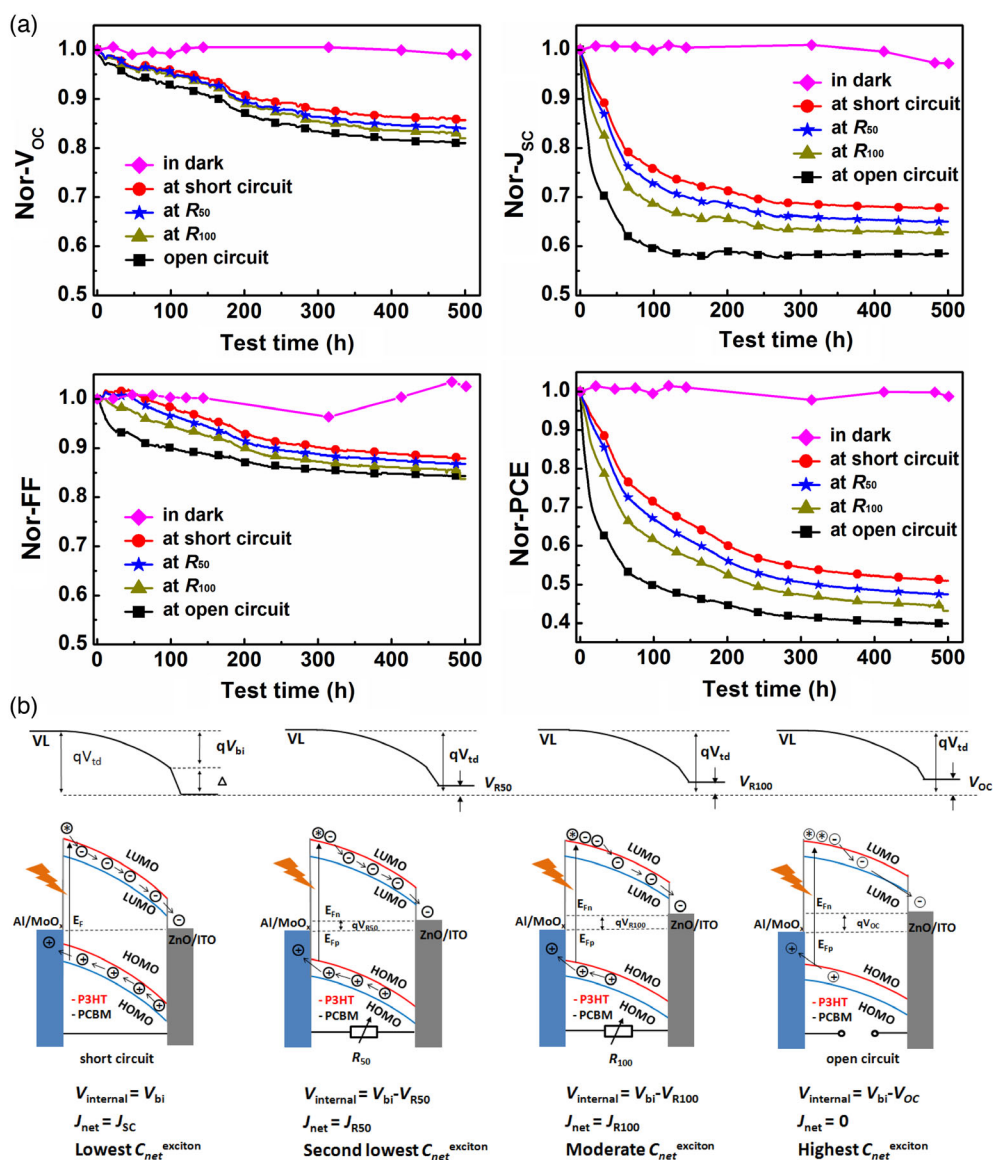


**Figure 10.** a) External load-dependent degradation of P3HT:PC<sub>61</sub>BM solar cells and b) the corresponding energy band alignment of the photoactive layer under different load conditions. Adapted with permission.<sup>[75]</sup> Copyright 2017, Royal Society of Chemistry.

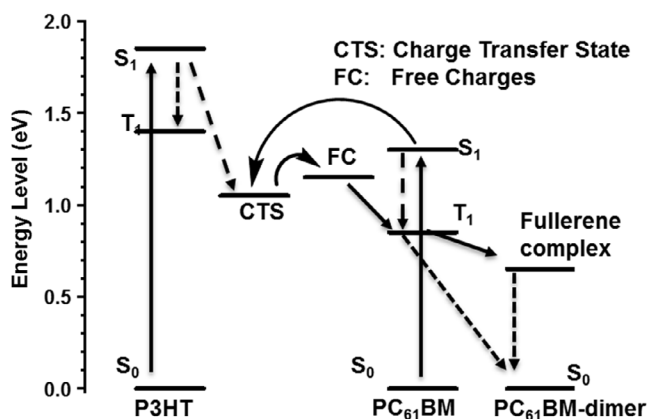


**Figure 11.** Proposed energy diagram of P3HT:PC<sub>61</sub>BM under light illumination. Formation of PC<sub>61</sub>BM dimer is directly related to the triplet state of PC<sub>61</sub>BM.

Based on the understanding of the mechanism of fullerene dimerization, we first reported using piperazine as the stabilizer in PFSCs.<sup>[75,150,151]</sup> This is based on the understanding that organic amine can quench the triplet of fullerene molecules.<sup>[152]</sup> Our experiment confirmed that piperazine doping can be applied to different PFSCs, including P3HT:PC<sub>61</sub>BM, PTB7-Th:PC<sub>61</sub>BM and poly[(5,6-difluoro-2,1,3-benzothiadiazol-4,7-diyl)-alt-(3,3''-di(2-octyldodecyl)-2,2',5',2'',5'',2'''-quaterthiophen-5,5'''-diyl)] (PffBT4T-2OD):PC<sub>61</sub>BM.<sup>[150]</sup> Detailed analysis with electron spin resonance spectroscopy (ESR) and transient current technology (CELIV) confirmed that piperazine doping is able to increase the concentration of fullerene anions in the photoactive layers, which is originated from the photon-induced electron transfer between piperazine and fullerene molecules<sup>[150]</sup> (Figure 12). By systematically investigating the influence of the molecular structure of piperazine derivatives on the stabilization effect of the piperazine compounds, we proved that the N–H is the essential unit that brings the piperazine closer to fullerene molecule through intermolecular H-bonding (Figure 13).<sup>[151]</sup> It is worth pointing out that as a cheap and often used material for electron buffer layer of PSCs, PEI also has excellent stability enhancement effects.<sup>[153]</sup>

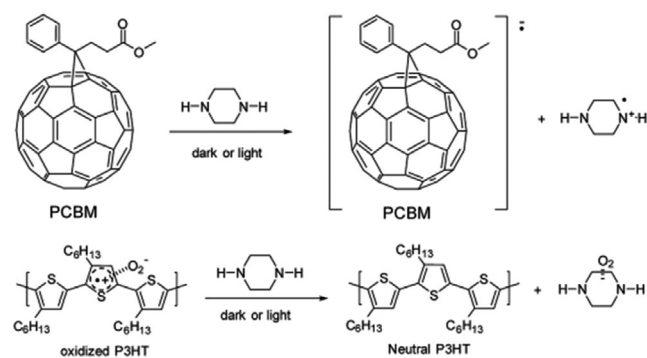


**Figure 12.** Molecular interaction of piperazine with PC<sub>61</sub>BM and P3HT. Adapted with permission.<sup>[150]</sup> Copyright 2019, Royal Society of Chemistry.

In addition, Li and co-workers reported that in the case of unencapsulated environment, the triplet fullerene excitons are easily quenched by oxygen to generate highly reactive singlet oxygen, which will cause severe photooxidation of the PC<sub>61</sub>BM.<sup>[154]</sup> Moreover, Durrant and co-workers<sup>[155]</sup> and Turkovic et al.<sup>[71]</sup> found that fullerene or polymer triplets can sensitize singlet oxygen which then further initiate the radical oxidation chain, resulting in performance degradation of PSCs. Therefore, whether in an inert atmosphere or in the air, triplet fullerene excitons have a negative impact on the performance of PFSCs.

### 3.3.2. Morphological Change

Except for the fullerene dimerization, the changes in nanomorphology of the photoactive layer is another key factor leading to the performance decay. The morphological changes in the photoactive layer are mainly due to two reasons. On the one hand, high-temperature heating causes excessive crystallization or aggregation of the polymer or fullerene,<sup>[47,156]</sup> and on the other hand, the severe phase separation of the polymer and fullerene due to their poor compatibility.<sup>[49,157]</sup> Excessive changes in the morphology of PSCs will damage the interpenetrating network structure of bulk heterojunction, thereby reducing the effective contact area, which will hinder the separation and transmission of charges, and ultimately cause degradation of device performance.<sup>[158]</sup>

When a PSC is exposed to the sunlight under operation, the surface temperature can reach up to 80 °C. Such a high temperature will unavoidably change the morphology of the photoactive layer. The effect of thermal heating on device performance has two sides. When polymer film is heated at a temperature higher than its glass transition temperature ( $T_g$ ), the polymer might crystallize, yielding highly crystalline phase, which helps in achieving high charge-carrier mobility. For example, Ocko and co-workers found that only when annealing at a high temperature higher than the  $T_g$  of poly[[9-(1-octylnonyl)-9H carbazole-2,7-diyl]-2,5-thiophenediyl-2,1,3-benzothiadiazole-4,7-diyl-2,5-thiophenediyl] (PCDTBT), a unique bilayer crystalline structure can be obtained, which has high crystallinity and mobility.<sup>[159]</sup> However, long-time thermal annealing would also lead to the over-crystallization of the polymer blend, which would reduce the performance of the cells. McGehee and co-workers found that both P3HT:PC<sub>61</sub>BM and PCDTBT:PC<sub>71</sub>BM solar cells exhibit a thermal degradation begin at their  $T_g$ .<sup>[47]</sup> They proved that due to the increased mobility of the polymer at high temperature, it will adhere to the back contact to form an electron blocking layer, which ultimately leads to a  $V_{OC}$  decay of device. Bertho et al. found that when heated at 110 °, the low- $T_g$  MDMO-PPV:PC<sub>61</sub>BM film formed clear large-scale PC<sub>61</sub>BM crystals, whereas the high- $T_g$  MDMO-PPV:PC<sub>61</sub>BM film hardly formed crystals.<sup>[156]</sup>

The increase in polymer mobility above  $T_g$  not only promotes the migration and crystallization of the polymer but also accelerates the aggregation or crystallization of fullerenes.<sup>[160–162]</sup> The exciton diffusion length of organic semiconductors is typically 5–10 nm.<sup>[163,164]</sup> Therefore, the ideal donor–acceptor phase separation within the photoactive layer should be few nanometers. However, the size of fullerene crystals formed at high

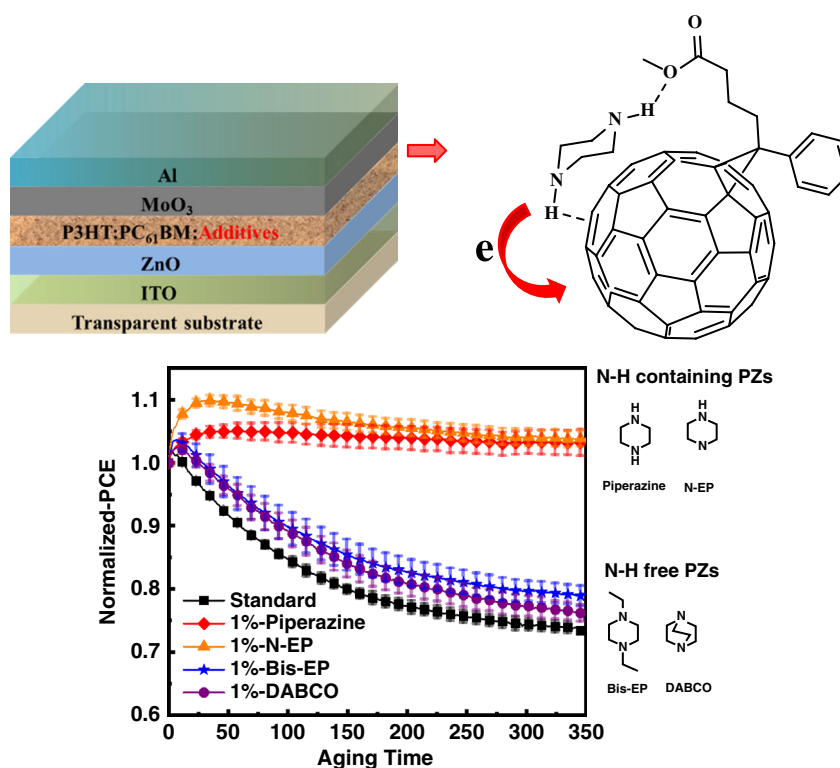


**Figure 13.** Stabilization effect of piperazine in PFSCs, the key H-bonding between fullerene and piperazine molecules. Adapted with permission.<sup>[151]</sup> Copyright 2020, American Chemical Society.

temperatures can even reach micrometer size, which seriously affects the electron transfer and charge separation within the PSCs. The continuous crystallization of fullerene molecules will then result in significant degradation of the device performance. Müller and co-workers studied the effect of temperature on the crystallization of PC<sub>71</sub>BM, and the results showed that when the heating temperature is lower than the  $T_g$  of the polymer,

the crystallization of PC<sub>61</sub>BM is inhibited, whereas crystallization of PC<sub>71</sub>BM dramatically when the sample is heated above the  $T_g$  of the polymer.<sup>[160]</sup> Durrant and co-workers also confirmed the same results (Figure 14). Interestingly, they found that short-term illumination of the photoactive layer is beneficial to inhibit the crystallization of PC<sub>61</sub>BM, which was ascribed to the formation of PC<sub>61</sub>BM dimmers.<sup>[41]</sup> It is worth pointing

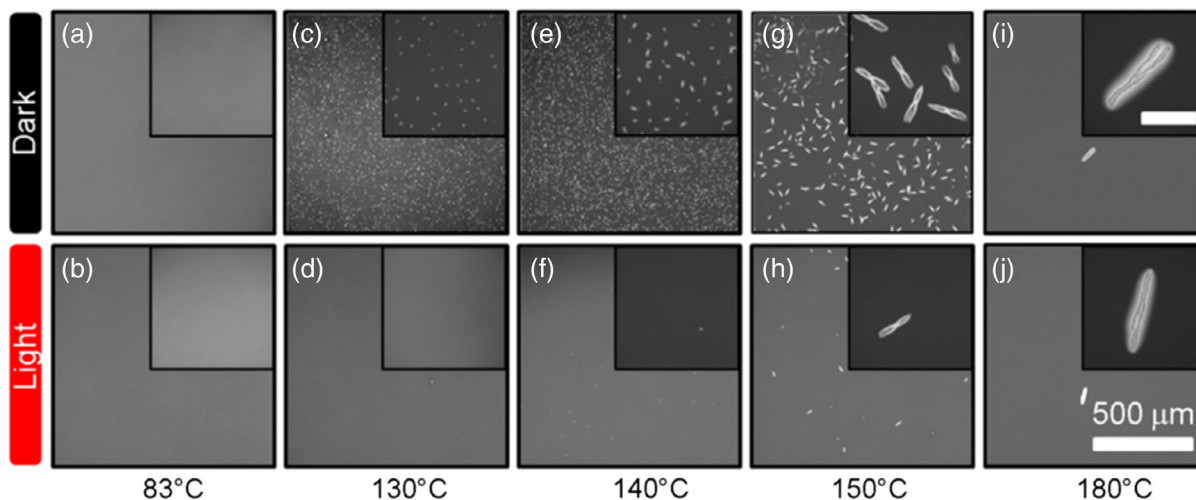


**Figure 14.** SEM diagrams of PC<sub>61</sub>BM crystals under different heating temperatures in dark and illumination environment. Adapted with permission.<sup>[41]</sup> Copyright 2014, Royal Society of Chemistry.

out that high-temperature heating can promote the dissociation of PC<sub>61</sub>BM dimer. Therefore, heating the photoactive polymer layer will eventually lead to the performance decay of the cell. Our recent research work on the thermal stability of P3HT:PC<sub>61</sub>BM solar cells found that moderate high-temperature heating can promote the dissociation of PC<sub>61</sub>BM dimers and make PSCs achieve ultrahigh thermal stability, whereas higher temperature heating will cause serious performance decay of PSCs.<sup>[165]</sup>

The morphology change in the photoactive layer was not only found for the film under thermal heating, donor–acceptor demixing in the PffBT4T-2OD:PC<sub>61</sub>BM solar cells was also found even they are kept at room temperature (Figure 15).<sup>[49]</sup> This is ascribed to the low miscibility of the donor and acceptor molecules, which will cause the spontaneous phase separation of the photoactive layer even in solid-state. Furthermore, Li and co-workers proposed to use spinodal interaction parameter  $\chi_{\text{spinodal}}$  to quantify the calculate the miscibility of the donor and acceptor materials in PSCs. Interestingly, the authors also found that piperazine doping is able to stabilize the mixed amorphous phases and finally improved the stability of solar cells.<sup>[157]</sup>

McGehee and co-workers found that crystalline polymer donors exhibit higher stability than amorphous polymers.<sup>[166]</sup> The high degree of crystallinity is beneficial to inhibit the formation of the traps in the photoactive layer and can also prevent the polymer from being oxidized. To solve the problem that the introduction of diiodooctane (DIO) additives will lead to the instability of PSCs, Chen and co-workers used a halogen-free solvent 1,4-butanedithiol (BT) to replace DIO as additive of PTB7-Th:PC<sub>71</sub>BM solar cells.<sup>[167]</sup> The use of BT can increase the  $T_g$  of PTB7-Th and finally effectively improve the device's stability. Muller reviewed the influence of polymer molecular structure on its  $T_g$ , and finally pointed out that polymer donor should have a moderate  $T_g$ , to realize flexible device preparation and application of PSCs.<sup>[168]</sup> The  $T_g$  of polymer donor should be less than the experimental annealing temperature to optimize the morphology of the photoactive layer by the thermal annealing process, and a higher  $T_g$  is also required to ensure higher device stability. Therefore, it is necessary to consider the processing temperature and the stability of PSCs while increasing the  $T_g$  of the polymer donors.

In addition to using high  $T_g$  polymer, scientists found that ternary approach can also improve the morphological stability of the photoactive layer of PSCs. The original intention of the ternary approach was to broaden the absorption spectrum of the photoactive layer to improve the efficiency of PSCs, but it was surprising and pleasant to find that the construction of the ternary photoactive layer structure can also stabilize the morphology and structure of the photoactive layer at the same time, and finally realize the stability improve of device. Chen et al. designed a 1D/2A ternary system (PBDB-T:PC<sub>71</sub>BM: 3,9-bis(2-methylene-(3-(1,1-dicyanomethylene)-indanone))-5,5,11,11-tetrakis(4-hexylphenyl)-dithieno[2,3-d:2',3'-d']-s-indaceno[1,2-b:5,6-b']dithiophene (ITIC)) PSC. This ternary structure results in cascade energy levels, broadened light-harvesting, modulated electron mobility, high exciton dissociation, and reduced recombination, which ultimately effectively improves device performance.<sup>[169]</sup> More importantly, the photoactive layer of the ternary structure has a wide thickness tolerance (200–510 nm), and has better thermal stability than each binary device. Yang and co-workers introduced an n-type poly[(N,N'-bis(2-octyldecyl)-naphthalene-1,4,5,8-bis(dicarboximide)-2,6-diyil)-alt-5,5-(2,2-bithiophene)] (P(NDI2OD-T2)) macromolecular additive to the photoactive layer of PTB7-Th:PC<sub>71</sub>BM solar cells, which on the one hand improves the device performance; on the other hand, it locks the morphology of the photoactive layer and greatly improves the stability of device.<sup>[170,171]</sup> Shen and co-workers introduced a nonfullerene acceptor IDT-OT into the PBDB-T:PC<sub>71</sub>BM binary blend system PSCs to form a stable alloy acceptor structure, which effectively improve both the performance and thermal stability of PSCs.<sup>[172]</sup> Another novel strategy is to construct molecular lock structure to stabilize the morphology of the photoactive layer. Zhan and co-workers doped a 4,4'-Biphenol (BPO) small molecule into the photoactive layer. The doped BPO can be connected to the F-containing polymer donors through hydrogen bonding to form a molecular lock structure (Figure 16), which simultaneously inhibits the excessive aggregation of polymers and fullerenes, and ultimately improves the device stability.<sup>[173]</sup> In addition, recent studies have also shown that the ternary approach can also effectively improves the stability of PNFSCs. For example, Zhang and co-workers designed a 2D/1A ternary system

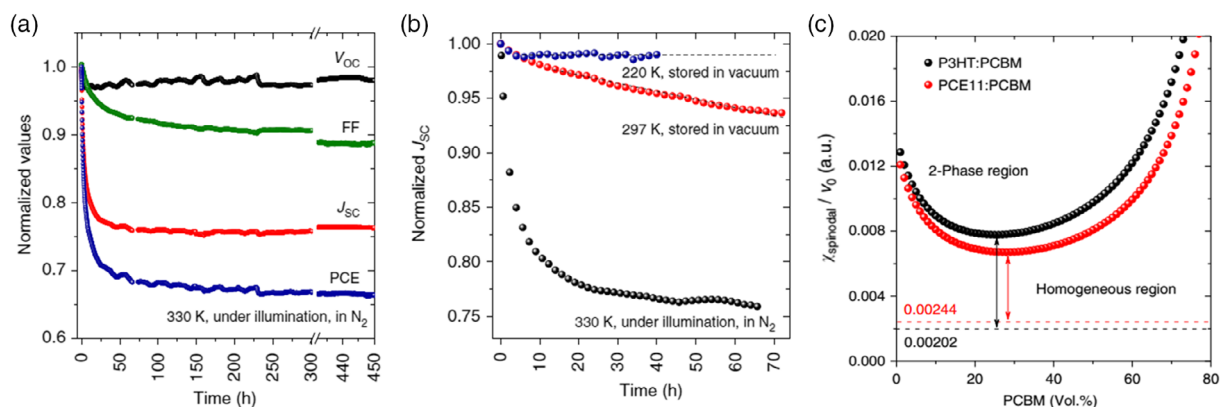


**Figure 15.** a) Degradation of PffBT4T-2OD:PC<sub>61</sub>BM cells under continuous light illumination; b) decay of  $J_{\text{sc}}$  of the cell at different conditions; c) polymer donor/PC<sub>61</sub>BM liquid (melt) solid transition diagrams. Reproduced with permission under the terms of the Creative Commons CC BY license.<sup>[49]</sup> Copyright 2017, the Authors. Published by Nature Communications.

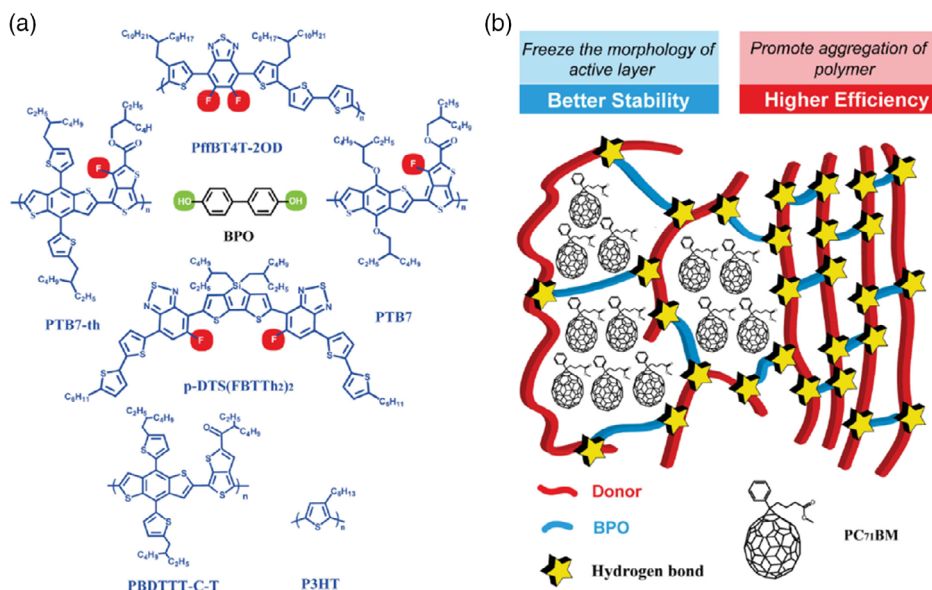


**Figure 16.** a) Molecular structures of PTB7, PTB7-th, PffBT4T-2OD, p-DTS(FBTTh<sub>2</sub>)<sub>2</sub>, PBDTTT-C-T, P3HT, and BPO. b) Doping BPO to construct a molecular lock structure to stabilize the morphology of the photoactive layer. Reproduced with permission.<sup>[173]</sup> Copyright 2016, WILEY-VCH.

(poly[4,8-bis(5-(2-ethylhexyl)thiophen-2-yl)benzo[1,2-*b*;4,5-*b*0]-dithiophene-2,6-diyl-alt-(4-(2-ethylhexyl)-3-fluorothiopheno[3,4-*b*]-thiophene)-2-carboxylate-2,6-diyl] (PBDTTT-ET-T):PCDTBT:ITIC) solar cells.<sup>[174]</sup> The optimized ternary system broadens the photon harvesting and stabilizes the morphology of photoactive layer, thereby simultaneously improving the performance and air stability of PSCs. Recently, we also designed a ternary system (PBDB-T:ITIC: (5Z,50Z)-5,5 0-((7,7 0-(9,9-dioctyl-9*H*-fluorene-2,7-diyl)bis(benzo[*c*]1,2,5) thiadiazole-7,4-diyl))-bis(methanylylidene))bis(3-ethyl-2-thioxothiazolidin-4-one) (FBR)) solar cell based on a acceptor alloy structure (ITIC:FBR).<sup>[175]</sup> The introduced FBR and ITIC form an alloy structure, which not only increase the  $V_{OC}$  but also effectively improve the stability of PSCs. These results proved that the ternary strategy has an effective stability improvement effect for both PFSCs and PNFSCs.

### 3.3.3. High Boiling Point Solvent

DIO is an additive commonly used in fullerene-based PSCs to adjust the morphology to achieve a high PCE.<sup>[15,176,177]</sup> However, many precious studies have reported that after doping with DIO, various PSCs, including PBDTTTEFT:PC<sub>71</sub>BM,<sup>[178]</sup> PTB7-PC<sub>71</sub>BM,<sup>[179,180]</sup> PTB7-Th:PC<sub>71</sub>BM, and PBDBT:PC<sub>71</sub>BM<sup>[181]</sup> show poor stability. In the early stage, it is believed that the short thermal annealing cannot remove the residual DIO in the photoactive layer due to its higher boiling point. Recently, Kopidakis and co-workers proved that the residual DIO in photoactive layer can act as a radical initiator to accelerate the photo-oxidation process of the polymer donor (**Figure 17**).<sup>[180]</sup> Treating the polymer blend with high-temperature annealing (170 °/30 min) or under high vacuum can effectively remove DIO, which significantly improves the stability of PSCs. Moreover, Heumueller and co-workers recently discovered that DIO decomposed under ultraviolet light, which produce free radicals and

react with PC<sub>71</sub>BM, causing the degradation of device performance (**Figure 18**).<sup>[182]</sup> Knowing that the residual DIO might initiate the decomposition of conjugated polymers, eliminating DIO in photoactive layer or replacing light-stable additives should be one way to improve the stability of solar cells. For example, Chen and co-workers used a halogen-free solvent BT to replace DIO as additive of PTB7-Th:PC<sub>71</sub>BM solar cells, which ultimately effectively improved the stability of PSCs.<sup>[167]</sup>

### 3.3.4. Energy Disorder

Numerous studies reported that the photoinduced  $V_{OC}$  loss of PSCs is related to the energy disorder of the photoactive layer, especially for PSCs based on amorphous polymers.<sup>[146,183]</sup> In the early stage, there are two possible mechanism responsible for the photoinduced  $V_{OC}$  loss of PSCs (**Figure 19**). The first mechanism is that continuous illumination induce the increased trap-assisted recombination in the photoactive layer, which reduces the charge-carrier density and leads to a decrease in  $V_{OC}$  of PSCs. The second mechanism is that the density of states (DOS) of photoactive layer broadens during the PSCs aging process, while the carrier density is unchanged. In this way, the

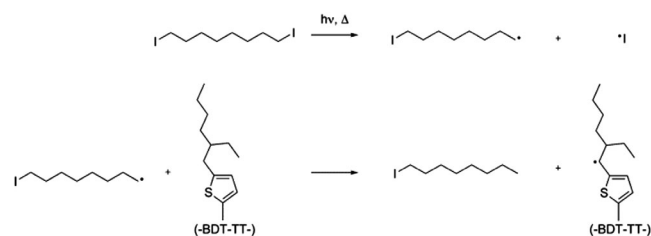


**Figure 17.** Photolysis of DIO and the reaction of decomposition of DIO with polymer donor. Adapted with permission.<sup>[180]</sup> Copyright 2016, American Chemical Society.

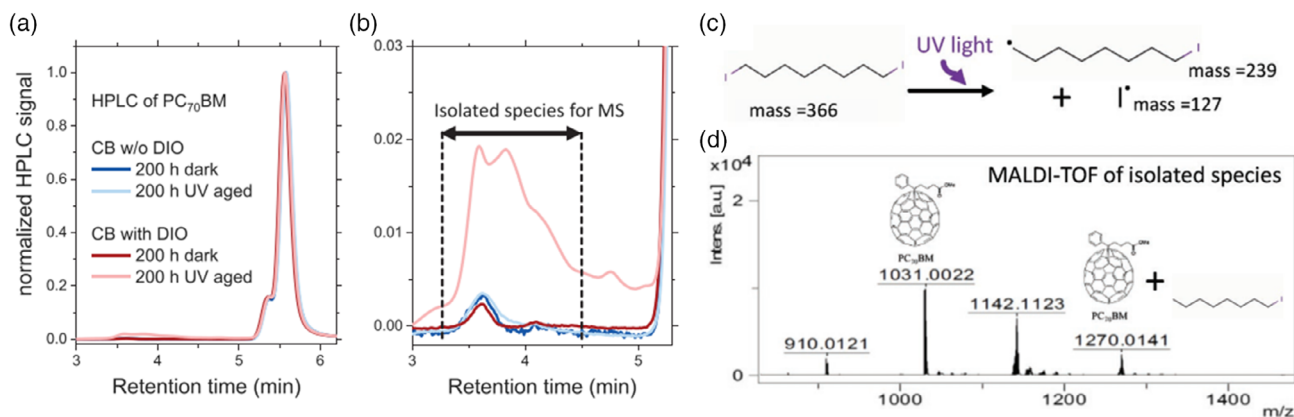


**Figure 18.** a) HPLC elograms for DIO-processed and b) UV-aged layers reveal new chemical compounds. c) The photodecomposition of DIO produces free radicals and d) reacts with PC<sub>71</sub>BM. Reproduced with permission.<sup>[182]</sup> Copyright 2019, WILEY-VCH.

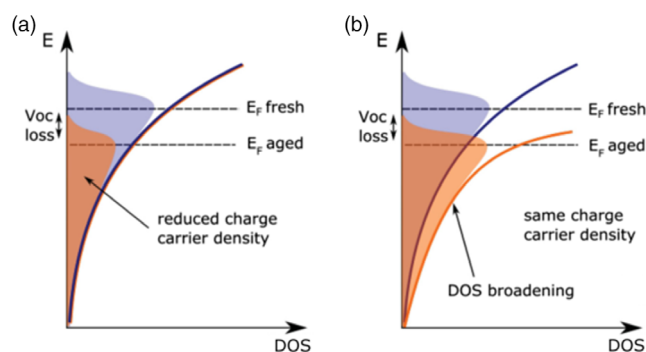


**Figure 19.** a,b) Two aging pathways leading to the  $V_{OC}$  loss of PSCs. Reproduced with permission.<sup>[183]</sup> Copyright 2015, WILEY-VCH.

widened DOS filled with the same number of carrier will cause a loss in  $V_{OC}$ . In view of this, McGehee and co-workers compared the recombination rate, carrier densities, and DOS of PCDTBT:PC<sub>71</sub>BM solar cells before and after aged and proved that the photoinduced  $V_{OC}$  loss of PSCs is caused by a redistribution of charge carriers in a broader DOS.<sup>[146]</sup> Furthermore, they found that PSCs based on crystalline materials with high carrier density are more stable against disorder-induced  $V_{OC}$  loss, which were also proved in their another work.<sup>[166]</sup> In addition, Durrant and co-workers reported that the burn-in degradation of the PffBT4T-2OD:PC<sub>71</sub>BM solar cell is related to the trap-state formation of the photoactive layer, and using nonfullerene acceptor can inhibit the formation of trap states in the photoactive layer.<sup>[184]</sup> In general, a lot of studies have shown that trap states in the photoactive layer will increase the DOS, which is considered to be the main reason for the decay of PSCs, especially for the  $V_{OC}$  loss,<sup>[183,185,186]</sup> and using highly crystalline polymer donors or nonfullerene acceptors can suppress the disorder-induced device decay.

### 3.3.5. Other Factors that Influence the Stability of PSCs

**Fullerene Radicals:** Gao and co-workers found that continuous illumination causes the oxidation of PC<sub>71</sub>BM in the poly [2,3-bis-(3-octyloxyphenyl)quinoxaline-5,8-diyl-altthiophene-2,5-diyl]

(TQ1):PC<sub>71</sub>BM solar cells, which not only leads to the recombination of charges but also leads to energetic disorder, and finally causes the  $V_{OC}$  decay of device.<sup>[187]</sup> Moreover, Troshin and co-workers found that the dimerization of PC<sub>61</sub>BM in the encapsulated PCDTBT:PC<sub>61</sub>BM solar cells has little effect on the performance of the solar cells.<sup>[40]</sup> After comparative experiments, they believed that the generation of light-induced fullerene radicals might be another reason for the degradation of PSCs.

**Impurities in the Polymers:** Although various purification steps have been carried out during the preparation of polymer materials, trace amount of palladium-, tin-, and halogen-containing impurities will inevitably remain within the final polymer products.<sup>[188–190]</sup> Also the plastic syringes used for the preparation of polymer solution for cells fabrication will introduce silicone and siloxane impurities into the photoactive layer as well.<sup>[191,192]</sup> These impurities will affect the initial performance and also the stability of the cells. For example, Camaioni et al. reported that the residual palladium comes from polymerization/purification process will reduce the hole mobility of the polymer donor poly{[40-(9,9-bis(2-ethylhexyl)fluoren-2-yl)-20,10,30-benzothiadiazole-7,70-diyl]-co-[20-(9,9-bis(2-ethylhexyl)fluoren-2-yl)thien-7,50-diyl]} (PFB-co-FT), and also decrease the device performance of PSCs based on PFB-co-FT:PC<sub>61</sub>BM blends.<sup>[193]</sup> Rivaton and co-workers found that low-regioregular P3HT with high number of impurities is more likely to be photooxidized than crystalline P3HT. The photooxidation of P3HT leads to the formation of low-molecular-weight carboxylic acids, which can diffuse and migrate out of the polymer films, resulting the poor performance of P3HT film.<sup>[194]</sup> Ohkita and co-workers studied the light-induced degradation of P3HT:ICBA solar cells and found that bromine residuals at P3HT chain ends leads to the formation of trap sites in P3HT domains, which decrease the charge collection of photoactive layer and ultimately caused the degradation of device performance.<sup>[39]</sup> The research results of McGehee have further proved these results. Using size exclusion chromatography (SEC) to remove low-molecular weight species of poly (benzo [1, 2-*b'*: 4, 5-*b'*] dithiophene-thieno [3, 4-*c'*] pyrrole-4, 6-dione) (PBDDTPD) in the photoactive layer can significantly improve the shelf stability of  $J_{SC}$  of device.<sup>[46]</sup> In view of the serious negative effects of residual impurities on the efficiency and stability of PSCs, it is of great

significance to develop a method for detecting impurities. Therefore, Darling and co-workers reported a method for tracing impurities in PSCs using synchrotron-based X-ray fluorescence, which can not only to identify which impurities are present but also to quantitatively measure their concentration.<sup>[195]</sup>

#### 4. Conclusion and Outlook

In summary, based on the research results on the degradation of PFSCs, we can classify the degradation processes of PSCs into two different types: the extrinsic and the intrinsic degradation processes. The extrinsic degradation processes of PSCs are mainly ascribed to the chemical reaction of water and oxygen with various functional layers. Blocking the reactive water and oxygen from the cell with proper encapsulation is the most effective way to suppress the extrinsic degradation processes. In contrast, the intrinsic degradation of PSCs induced by light illumination, thermal heating, and electronic bias are more complicated and they cannot be suppressed by external encapsulation. As the intrinsic degradation process will determine the longest lifetime of PSCs, it is more important to understand the intrinsic degradation mechanism and to find a way to improve the intrinsic stability.

As summarized in Table 2, intrinsic degradation of PSCs might happen to the electrode, the buffer layer, and the photoactive layers. Interface atoms or molecules diffusion is the most significant pathway for the degradation of the electrode and the buffer layers, which could on the one hand cause the change of work functions of these two layers, on the other hand yield more pronounced interfacial charge recombination. Using a more stable carbon electrode or with proper interfacial modification could partially solve the problem. However, as the layer thickness of the

buffer is limited to dozens of nanometer, developing an efficient interfacial layer with high working thickness could be another solution for this issue.

There are several decay pathways for the photoactive layer of the PSC when it is under operation. Light-induced dimerization, morphology change of the photoactive layer, photochemical decomposition initiated by the residue high boiling point solvent, broadening of the DOS are among the most important degradation pathways for the photoactive layer. Dimerization of fullerene molecules under light illumination was proved to be one of the main intrinsic degradation pathways for the PFSCs. The dimerization of fullerene is fullerene triplet correlated process. Therefore, using organic amine to quench the high-energy triple state of fullerene is an effective way to solve this problem. Improving the nanomorphology stability of the polymer blend using high  $T_g$  polymers, ternary organic blend systems, as well as cross-linkable materials, could be the way to solve this issue. As the residue halogenated additive might cause the degradation of the photoactive layer as well, avoiding using these solvent additives or completely removing the additive is highly recommended.

Overall, the experiences learned from the PFSCs are highly helpful in understanding the degradation of the PNFSCs. Although no photon dimerization can be found in the nonfullerene acceptor, other degradation pathways, such as interfacial degradation, morphology changes, and chemical decomposition of the photoactive layer caused by the solvent additives, could be found as well in the nonfullerene solar cells. It is highly expectable that the stability of the PNFSCs can also be improved after understanding the specific degradation pathways of these high-performance solar cells. Therefore, in our opinion, to improve the stability of PNFSCs, we must first understand their degradation mechanism by investigating their aging behavior, and then

**Table 2.** Summary of intrinsic degradation and solution strategies of each functional layer of PFSCs.

Functional layer of PSCs	Aging factors	Resolution strategy
Top metal electrode	Migration of metal (Ag, Al) atoms	Searching for electric-field insensitive top electrode, such as carbon electrodes
Electrode buffer layer	Li <sup>+</sup> of LiF diffuse into the photoactive layer; ZnO contains many defects	Replace or modify the unstable cathode buffer materials
Anode buffer layer	Highly acidic PEDOT:PSS corrode the ITO electrode; PSS of PEDOT:PSS undergo phase separation and even diffuse into photoactive layer; MoO <sub>3</sub> reacts with Ag electrodes under heating; light-induced reduction reaction of MoO <sub>3</sub> ;	Replace anode buffer materials or insert a barrier layer
Photoactive layer	Triplet excitons related fullerene dimerization Morphological change	Fullerene triplet passivator doping or using nonfullerene acceptor Using polymer donor with high $T_g$ and crystallinity; constructive a stable BHJ structure; ternary approach
	High boiling point solvent	Eliminating high boiling point solvent in photoactive layer or replacing light-stable additives
	Energy disorder	Using of high-crystalline polymer or nonfullerene acceptor
Other factors	Fullerene radicals	Doping stabilizing additives or using nonfullerene
	Impurities in the polymer	Purification of polymers
	...	...

block their aging path from both the interface layer and the photoactive layer based on their degradation mechanism.

## Acknowledgements

The authors acknowledge the financial support from the Chinese Academy of Science (No. YJKYYQ20180029), National Natural Science Foundation of China (22075315, 61904121), China Postdoctoral Science Foundation (2020M681756), Postdoctoral Science Foundation and **Natural Science Foundation of Shanxi Province (201801D221136)**.

## Conflict of Interest

The authors declare no conflict of interest.

## Keywords

degradation pathways, fullerene acceptors, polymer solar cells, stability improvement, stress factors

Received: October 18, 2020

Revised: January 19, 2021

Published online:

- 
- [1] Y. Li, G. Xu, C. Cui, Y. Li, *Adv. Energy Mater.* **2018**, *8*, 1701791.  
 [2] T. Stubhan, H. Oh, L. Pinna, J. Krantz, I. Litzov, C. J. Brabec, *Org. Electron.* **2011**, *12*, 1539.  
 [3] K. Zhang, Z. C. Hu, C. Sun, Z. H. Wu, F. Huang, Y. Cao, *Chem. Mater.* **2017**, *29*, 141.  
 [4] R. Xue, J. Zhang, Y. Li, Y. Li, *Small* **2018**, *14*, 1801793.  
 [5] Y. Cui, H. Yao, T. Zhang, L. Hong, B. Gao, K. Xian, J. Qin, J. Hou, *Adv. Mater.* **2019**, *31*, 1904512.  
 [6] J. Kettle, N. Bristow, T. K. N. Sweet, N. Jenkins, G. A. dos Reis Benatto, M. Jørgensen, F. C. Krebs, *Energy Environ. Sci.* **2015**, *8*, 3266.  
 [7] K.-S. Chen, J.-F. Salinas, H.-L. Yip, L. Huo, J. Hou, A. K. Y. Jen, *Energy Environ. Sci.* **2012**, *5*, 9551.  
 [8] L. K. Reb, M. Böhmer, B. Predeschly, S. Grott, C. L. Weindl, G. I. Ivandekic, R. Guo, C. Dreißigacker, R. Gernhäuser, A. Meyer, P. Müller-Buschbaum, *Joule* **2020**, *4*, 1880.  
 [9] Q. Liu, Y. Jiang, K. Jin, J. Xu, W. Li, J. Xiong, J. Liu, Z. Xiao, K. Sun, S. Yang, X. Zhang, L. Ding, *Sci. Bull.* **2020**, *65*, 272.  
 [10] Y. Lin, Y. Firdaus, F. H. Isikgor, M. I. Nugraha, E. Yengel, G. T. Harrison, R. Hallani, A. El-Labban, H. Faber, C. Ma, X. Zheng, A. Subbiah, C. T. Howells, O. M. Bakr, I. McCulloch, S. D. Wolf, L. Tsetseris, T. D. Anthopoulos, *ACS Energy Lett.* **2020**, *5*, 2935.  
 [11] H. W. Kroto, J. R. Heath, S. C. O'Brien, R. F. Curl, R. E. Smalley, *Nature* **1985**, *318*, 162.  
 [12] G. Yu, J. Gao, J. C. Hummelen, F. Wudl, A. J. Heeger, *Science* **1995**, *270*, 1789.  
 [13] G. Li, V. Shrotriya, J. S. Huang, Y. Yao, T. Moriarty, K. Emery, Y. Yang, *Nat. Mater.* **2005**, *4*, 864.  
 [14] D. Mühlbacher, M. Scharber, M. Morana, Z. G. Zhu, D. Waller, R. Gaudiana, C. Brabec, *Adv. Mater.* **2006**, *18*, 2884.  
 [15] Y. Y. Liang, Z. Xu, J. B. Xia, S. T. Tsai, Y. Wu, G. Li, C. Ray, L. P. Yu, *Adv. Mater.* **2010**, *22*, E135.  
 [16] Q. P. Fan, W. Y. Su, Y. Wang, B. Guo, Y. F. Jiang, X. Guo, F. Liu, T. P. Russell, M. J. Zhang, Y. F. Li, *Sci. China Chem.* **2018**, *61*, 531.  
 [17] J. B. Zhao, Y. K. Li, G. F. Yang, K. Jiang, H. R. Lin, H. Ade, W. Ma, H. Yan, *Nat. Energy* **2016**, *1*, 15027.  
 [18] M. Lenes, G. J. A. H. Wetzelaer, F. B. Kooistra, S. C. Veenstra, J. C. Hummelen, P. W. M. Blom, *Adv. Mater.* **2008**, *20*, 2116.  
 [19] G. Zhao, Y. He, Y. Li, *Adv. Mater.* **2010**, *22*, 4355.  
 [20] Y. H. Liu, J. B. Zhao, Z. K. Li, C. Mu, W. Ma, H. W. Hu, K. Jiang, H. R. Lin, H. Ade, H. Yan, *Nat. Commun.* **2014**, *5*, 5293.  
 [21] Y. Yang, Z.-G. Zhang, H. Bin, S. Chen, L. Gao, L. Xue, C. Yang, Y. Li, *J. Am. Chem. Soc.* **2016**, *138*, 15011.  
 [22] S. S. Li, L. Ye, W. C. Zhao, S. Q. Zhang, S. Mukherjee, H. Ade, J. H. Hou, *Adv. Mater.* **2016**, *28*, 9423.  
 [23] W. C. Zhao, S. S. Li, H. F. Yao, S. Q. Zhang, Y. Zhang, B. Yang, J. H. Hou, *J. Am. Chem. Soc.* **2017**, *139*, 7148.  
 [24] W. C. Zhao, S. S. Li, S. Q. Zhang, X. Y. Liu, J. H. Hou, *Adv. Mater.* **2017**, *29*, 1604059.  
 [25] T. Yan, W. Song, J. Huang, R. Peng, L. Huang, Z. Ge, *Adv. Mater.* **2019**, *31*, 1902210.  
 [26] Y. Lin, B. Adilbekova, Y. Firdaus, E. Yengel, H. Faber, M. Sajjad, X. Zheng, E. Yarali, A. Seitkhan, O. M. Bakr, A. El-Labban, U. Schwingschögl, V. Tung, I. McCulloch, F. Laquai, T. D. Anthopoulos, *Adv. Mater.* **2019**, *31*, 1902965.  
 [27] Y. Sun, M. Chang, L. Meng, X. Wan, H. Gao, Y. Zhang, K. Zhao, Z. Sun, C. Li, S. Liu, H. Wang, J. Liang, Y. Chen, *Nat. Electron.* **2019**, *2*, 513.  
 [28] L. X. Meng, Y. M. Zhang, X. J. Wan, C. X. Li, X. Zhang, Y. B. Wang, X. Ke, Z. Xiao, L. M. Ding, R. X. Xia, H. L. Yip, Y. Cao, Y. S. Chen, *Science* **2018**, *361*, 1094.  
 [29] J. K. J. van Duren, X. Yang, J. Loos, C. W. T. Bulle-Lieuwma, A. B. Sieval, J. C. Hummelen, R. A. J. Janssen, *Adv. Funct. Mater.* **2004**, *14*, 425.  
 [30] X. Yang, J. K. J. van Duren, R. A. J. Janssen, M. A. J. Michels, J. Loos, *Macromolecules* **2004**, *37*, 2151.  
 [31] X. Yang, J. K. J. van Duren, M. T. Rispens, J. C. Hummelen, R. A. J. Janssen, M. A. J. Michels, J. Loos, *Adv. Mater.* **2004**, *16*, 802.  
 [32] S. Yamamoto, A. Orimo, H. Ohkita, H. Bente, S. Ito, *Adv. Energy Mater.* **2012**, *2*, 229.  
 [33] Y. Yao, J. Hou, Z. Xu, G. Li, Y. Yang, *Adv. Funct. Mater.* **2008**, *18*, 1783.  
 [34] H. Neugebauer, C. Brabec, J. C. Hummelen, N. S. Sariciftci, *Sol. Energy Mat. Sol. C* **2000**, *61*, 35.  
 [35] T. J. Savenije, J. E. Kroeze, X. Yang, J. Loos, *Adv. Funct. Mater.* **2005**, *15*, 1260.  
 [36] K. Feron, T. J. Nagle, L. J. Rozanski, B. B. Gong, C. J. Fell, *Sol. Energy Mat. Sol. C* **2013**, *109*, 169.  
 [37] K. Norrman, S. A. Gevorgyan, F. C. Krebs, *ACS Appl. Mater. Interfaces* **2009**, *1*, 102.  
 [38] A. J. Parnell, A. J. Cadby, A. D. F. Dunbar, G. L. Roberts, A. Plumridge, R. M. Dalgliesh, M. W. A. Skoda, R. A. L. Jones, *J. Polym. Sci. Part B: Polym. Phys.* **2016**, *54*, 141.  
 [39] Y. Tamai, H. Ohkita, M. Namatame, K. Marumoto, S. Shimomura, T. Yamanari, S. Ito, *Adv. Energy Mater.* **2016**, *6*, 1600171.  
 [40] L. N. Inasaridze, A. I. Shames, I. V. Martynov, B. Li, A. V. Mumyatov, D. K. Susarova, E. A. Katz, P. A. Troshin, *J. Mater. Chem. A* **2017**, *5*, 8044.  
 [41] H. C. Wong, Z. Li, C. H. Tan, H. L. Zhong, Z. G. Huang, H. Bronstein, I. McCulloch, J. T. Cabral, J. R. Durrant, *ACS Nano* **2014**, *8*, 1297.  
 [42] T. Heumueller, W. R. Mateker, A. Distler, U. F. Fritze, R. Cheacharoen, W. H. Nguyen, M. Biele, M. Salvador, M. von Delius, H. J. Egelhaaf, M. D. McGehee, C. J. Brabec, *Energy Environ. Sci.* **2016**, *9*, 247.  
 [43] A. Manor, E. A. Katz, T. Tromholt, F. C. Krebs, *Adv. Energy Mater.* **2011**, *1*, 836.  
 [44] G. Dennler, M. C. Scharber, C. J. Brabec, *Adv. Mater.* **2009**, *21*, 1323.

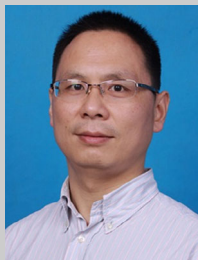
- [45] S. Schäfer, A. Petersen, T. A. Wagner, R. Kniprath, D. Lingenfeller, A. Zen, T. Kirchartz, B. Zimmermann, U. Würfel, X. Feng, T. Mayer, *Phys. Rev. B* **2011**, *83*, 165311.
- [46] W. R. Mateker, J. D. Douglas, C. Cabanetos, I. T. Sachs-Quintana, J. A. Bartelt, E. T. Hoke, A. El Labban, P. M. Beaujuge, J. M. J. Frechet, M. D. McGehee, *Energy Environ. Sci.* **2013**, *6*, 2529.
- [47] I. T. Sachs-Quintana, T. Heumüller, W. R. Mateker, D. E. Orozco, R. Cheacharoen, S. Sweetnam, C. J. Brabec, M. D. McGehee, *Adv. Funct. Mater.* **2014**, *24*, 3978.
- [48] W. R. Mateker, M. D. McGehee, *Adv. Mater.* **2017**, *29*, 1603940.
- [49] N. Li, J. D. Perea, T. Kassar, M. Richter, T. Heumueller, G. J. Matt, Y. Hou, N. S. Guedal, H. W. Chen, S. Chen, S. Langner, M. Berlinghof, T. Unruh, C. J. Brabec, *Nat. Commun.* **2017**, *8*, 14541.
- [50] M. Glatthaar, M. Riede, N. Keegan, K. Sylvester-Hvid, B. Zimmermann, M. Niggemann, A. Hinsch, A. Gombert, *Sol. Energy Mat. Sol. C* **2007**, *91*, 390.
- [51] V. S. Balderrama, M. Estrada, P. L. Han, P. Granero, J. Pallarés, J. Ferré-Borrull, L. F. Marsal, *Sol. Energy Mat. Sol. C* **2014**, *125*, 155.
- [52] K. Norrman, M. V. Madsen, S. A. Gevorgyan, F. C. Krebs, *J. Am. Chem. Soc.* **2010**, *132*, 16883.
- [53] T. He, J. N. Yao, *J. Photoch. Photobio. C* **2003**, *4*, 125.
- [54] S. Wilken, J. Parisi, H. Borchert, *J. Phys. Chem. C* **2014**, *118*, 19672.
- [55] P. Cheng, X. W. Zhan, *Chem. Soc. Rev.* **2016**, *45*, 2544.
- [56] M. Jørgensen, K. Norrman, S. Gevorgyan, T. Tromholt, B. Andreasen, F. Krebs, *Adv. Mater.* **2012**, *24*, 580.
- [57] A. Rivaton, A. Tournebize, J. Gaume, P.-O. Bussière, J.-L. Gardette, S. Therias, *Polym. Int.* **2014**, *63*, 1335.
- [58] A. Perthue, T. Gorisse, H. S. Silva, C. Lombard, D. Begue, P. Hudhomme, B. Pepin-Donat, A. Rivaton, G. Wantz, *J. Mater. Res.* **2018**, *33*, 1868.
- [59] S. B. Sapkota, A. Spies, B. Zimmermann, I. Dürr, U. Würfel, *Sol. Energy Mat. Sol. C* **2014**, *130*, 144.
- [60] P. Romero-Gomez, R. Betancur, A. Martinez-Otero, X. Elias, M. Mariano, B. Romero, B. Arredondo, R. Vergaz, J. Martorell, *Sol. Energy Mat. Sol. C* **2015**, *137*, 44.
- [61] T. Kim, J. H. Kang, S. J. Yang, S. J. Sung, Y. S. Kim, C. R. Park, *Energy Environ. Sci.* **2014**, *7*, 3403.
- [62] C. Y. Chang, F. Y. Tsai, *J. Mater. Chem.* **2011**, *21*, 5710.
- [63] A. Garg, S. K. Gupta, J. J. Jasieniak, T. B. Singh, S. E. Watkins, *Prog. Photovoltaics: Res. Appl.* **2015**, *23*, 989.
- [64] N. Chen, P. Kovacic, R. M. Howden, X. Wang, S. Lee, K. K. Gleason, *Adv. Energy Mater.* **2015**, *5*, 1401442.
- [65] N. Gasparini, M. Salvador, S. Strohm, T. Heumueller, I. Levchuk, A. Wadsworth, J. H. Bannock, J. C. de Mello, H. J. Egelhaaf, D. Baran, I. McCulloch, C. J. Brabec, *Adv. Energy Mater.* **2017**, *7*, 1700770.
- [66] J. L. Song, L. L. Ye, C. Li, J. Q. Xu, S. Chandrabose, K. K. Weng, Y. H. Cai, Y. P. Xie, P. O'Reilly, K. Chen, J. J. Zhou, Y. Zhou, J. M. Hodgkiss, F. Liu, Y. M. Sun, *Adv. Sci.* **2020**, 2001986.
- [67] X. Du, T. Heumueller, W. Gruber, A. Classen, T. Unruh, N. Li, C. J. Brabec, *Joule* **2018**, *2*, 1.
- [68] V. Turkovic, S. Engmann, N. Tsierekzos, H. Hoppe, U. Ritter, G. Gobsch, *ACS Appl. Mater. Interfaces* **2014**, *6*, 18525.
- [69] V. Turkovic, S. Engmann, N. Tsierekzos, H. Hoppe, M. Madsen, H. G. Rubahn, U. Ritter, G. Gobsch, *Appl. Phys. A* **2016**, *122*, 255.
- [70] V. Turkovic, S. Engmann, N. Tsierekzos, H. Hoppe, M. Madsen, H. G. Rubahn, U. Ritter, G. Gobsch, *J. Phys. D: Appl. Phys.* **2016**, *49*, 125604.
- [71] V. Turkovic, M. Prete, M. Bregnhøj, L. Inasaridze, D. Volyniuk, F. A. Obrezkov, J. V. Grazulevicius, S. Engmann, H.-G. Rubahn, P. A. Troshin, P. R. Ogilby, M. Madsen, *ACS Appl. Mater. Interfaces* **2019**, *11*, 41570.
- [72] T. M. Clarke, J. R. Durrant, *Chem. Rev.* **2010**, *110*, 6736.
- [73] J.-L. Brédas, J. E. Norton, J. Cornil, V. Coropceanu, *Acc. Chem. Res.* **2009**, *42*, 1691.
- [74] A. Distler, T. Sauermann, H. J. Egelhaaf, S. Rodman, D. Waller, K. S. Cheon, M. Lee, N. Drolet, D. M. Guldi, *Adv. Energy Mater.* **2014**, *4*, 1300693.
- [75] L. P. Yan, J. D. Yi, Q. Chen, J. Y. Dou, Y. Z. Yang, X. G. Liu, L. W. Chen, C. Q. Ma, *J. Mater. Chem. A* **2017**, *5*, 10010.
- [76] E. T. Hoke, I. T. Sachs-Quintana, M. T. Lloyd, I. Kauvar, W. R. Mateker, A. M. Nardes, C. H. Peters, N. Kopidakis, M. D. McGehee, *Adv. Energy Mater.* **2012**, *2*, 1351.
- [77] E. M. Speller, A. J. Clarke, J. Luke, H. K. H. Lee, J. R. Durrant, N. Li, T. Wang, H. C. Wong, J.-S. Kim, W. C. Tsoi, Z. Li, *J. Mater. Chem. A* **2019**, *7*, 23361.
- [78] E. M. Speller, A. J. Clarke, N. Aristidou, M. F. Wyatt, L. Francàs, G. Fish, H. Cha, H. K. H. Lee, J. Luke, A. Wadsworth, A. D. Evans, I. McCulloch, J.-S. Kim, S. A. Haque, J. R. Durrant, S. D. Dimitrov, W. C. Tsoi, Z. Li, *ACS Energy Lett.* **2019**, *4*, 846.
- [79] H. K. H. Lee, A. M. Telford, J. A. Röhr, M. F. Wyatt, B. Rice, J. Wu, A. de Castro Maciel, S. M. Tuladhar, E. Speller, J. McGettrick, J. R. Searle, S. Pont, T. Watson, T. Kirchartz, J. R. Durrant, W. C. Tsoi, J. Nelson, Z. Li, *Energy Environ. Sci.* **2018**, *11*, 417.
- [80] L.-M. Chen, Z. Hong, G. Li, Y. Yang, *Adv. Mater.* **2009**, *21*, 1434.
- [81] N. D. Treat, M. L. Chabinyc, *Ann. Rev. Phys. Chem.* **2014**, *65*, 59.
- [82] Y. Vaynzof, D. Kabra, L. Zhao, L. L. Chua, U. Steiner, R. H. Friend, *ACS Nano* **2011**, *5*, 329.
- [83] S. Engmann, C. R. Singh, V. Turkovic, H. Hoppe, G. Gobsch, *Adv. Energy Mater.* **2013**, *3*, 1463.
- [84] W. Ma, C. Yang, X. Gong, K. Lee, A. J. Heeger, *Adv. Funct. Mater.* **2005**, *15*, 1617.
- [85] Y. Ning, L. Lv, Y. Lu, A. Tang, Y. Hu, Z. Lou, F. Teng, Y. Hou, *Int. J. Photoenergy* **2014**, *2014*, 354837.
- [86] S. Bae, S. Kim, S.-W. Lee, K. J. Cho, S. Park, S. Lee, Y. Kang, H.-S. Lee, D. Kim, *J. Phys. Chem. Lett.* **2016**, *7*, 3091.
- [87] M. V. Khenkin, K. M. Anoop, E. A. Katz, I. Visoly-Fisher, *Energy Environ. Sci.* **2019**, *12*, 550.
- [88] M. V. Khenkin, E. A. Katz, A. Abate, G. Bardizza, J. J. Berry, C. Brabec, F. Brunetti, V. Bulović, Q. Burlingame, A. Di Carlo, R. Cheacharoen, Y.-B. Cheng, A. Colmann, S. Cros, K. Domanski, M. Dusza, C. J. Fell, S. R. Forrest, Y. Galagan, D. Di Girolamo, M. Grätzel, A. Hagfeldt, E. von Hauff, H. Hoppe, J. Kettle, H. Köbler, M. S. Leite, S. Liu, Y.-L. Loo, J. M. Luther, et al., *Nat. Energy* **2020**, *5*, 35.
- [89] E. Voroshazi, B. Verreet, A. Buri, R. Müller, D. Di Nuzzo, P. Heremans, *Org. Electron.* **2011**, *12*, 736.
- [90] S. Alborghetti, J. M. D. Coey, P. Stamenov, *Appl. Phys. Lett.* **2012**, *100*, 143301.
- [91] O. V. Molodtsova, I. M. Aristova, S. V. Babenkov, O. V. Vilkov, V. Y. Aristov, *J. Appl. Phys.* **2014**, *115*, 164310.
- [92] R. Rosch, D. M. Tanenbaum, M. Jørgensen, M. Seeland, M. Barenklau, M. Hermenau, E. Voroshazi, M. T. Lloyd, Y. Galagan, B. Zimmermann, U. Würfel, M. Hosel, H. F. Dam, S. A. Gevorgyan, S. Kudret, W. Maes, L. Lutsen, D. Vanderzande, R. Andriessen, G. Teran-Escobar, M. Lira-Cantu, A. Rivaton, G. Y. Uzunoglu, D. Germack, B. Andreasen, M. V. Madsen, K. Norrman, H. Hoppe, F. C. Krebs, *Energy Environ. Sci.* **2012**, *5*, 6521.
- [93] A. C. Hinckley, C. Wang, R. Pfattner, D. Kong, Y. Zhou, B. Ecker, Y. Gao, Z. Bao, *ACS Appl. Mater. Interfaces* **2016**, *8*, 19658.
- [94] M. Tavakkoli, R. Ajeian, M. Nakhaei Badrabadi, S. Saleh Ardestani, S. M. H. Feiz, K. Elahi Nasab, *Sol. Energy Mat. Sol. C* **2011**, *95*, 1964.
- [95] Y. Jiang, L. Sun, F. Jiang, C. Xie, L. Hu, X. Dong, F. Qin, T. Liu, L. Hu, X. Jiang, Y. Zhou, *Mater. Horizons* **2019**, *6*, 1438.
- [96] Y. H. Zhou, C. Fuentes-Hernandez, J. Shim, J. Meyer, A. J. Giordano, H. Li, P. Winget, T. Papadopoulos, H. Cheun, J. Kim, M. Fenoll, A. Dindar, W. Haske, E. Najafabadi, T. M. Khan, H. Sojoudi,

- S. Barlow, S. Graham, J. L. Bredas, S. R. Marder, A. Kahn, B. Kippelen, *Science* **2012**, 336, 327.
- [97] N. Kim, W. J. Potscavage, A. Sundaramoorthi, C. Henderson, B. Kippelen, S. Graham, *Sol. Energy Mat. Sol. C* **2012**, 101, 140.
- [98] Z. Wu, Z. Liu, Z. Hu, Z. Hawash, L. Qiu, Y. Jiang, L. K. Ono, Y. Qi, *Adv. Mater.* **2019**, 31, 1804284.
- [99] E. Calabrò, F. Matteocci, B. Paci, L. Cinà, L. Vesce, J. Barichello, A. Generosi, A. Reale, A. Di Carlo, *ACS Appl. Mater. Interfaces* **2020**, 12, 32536.
- [100] Z. Liu, P. You, S. Liu, F. Yan, *ACS Nano* **2015**, 9, 12026.
- [101] L. Yan, H. Gu, Z. Li, J. Zhang, Y. Yang, H. Wang, X. Liu, Z. Wei, Q. Luo, C.-Q. Ma, *Mater. Adv.* **2020**, 1, 1307.
- [102] H. Gu, L. Yan, S. Saxena, X. Shi, X. Zhang, Z. Li, Q. Luo, H. Zhou, Y. Yang, X. Liu, W. W. H. Wong, C.-Q. Ma, *ACS Appl. Energy Mater.* **2020**, 3, 9714.
- [103] L. S. Hung, C. W. Tang, M. G. Mason, *Appl. Phys. Lett.* **1997**, 70, 152.
- [104] Z. Yin, J. Wei, Q. Zheng, *Adv. Sci.* **2016**, 3, 1500362.
- [105] C. J. Brabec, S. E. Shaheen, C. Winder, N. S. Sariciftci, P. Denk, *Appl. Phys. Lett.* **2002**, 80, 1288.
- [106] S. O. Jeon, J. Y. Lee, *Sol. Energy Mat. Sol. C* **2012**, 101, 160.
- [107] F. Li, J. Zhao, K. Yao, Y. Chen, *Chem. Phys. Lett.* **2012**, 553, 36.
- [108] L. P. Yan, Y. Z. Yang, C. Q. Ma, X. G. Liu, H. Wang, B. S. Xu, *Carbon* **2016**, 109, 598.
- [109] M. Wang, Q. Tang, J. An, F. Xie, J. Chen, S. Zheng, K. Y. Wong, Q. Miao, J. Xu, *ACS Appl. Mater. Interfaces* **2010**, 2, 2699.
- [110] J.-H. Huang, M. A. Ibrahim, C.-W. Chu, *Prog. Photovoltaics: Res. Appl.* **2015**, 23, 1017.
- [111] J. Kim, H. Lee, S. J. Lee, W. J. da Silva, A. R. bin Mohd Yusoff, J. Jang, *J. Mater. Chem. A* **2015**, 3, 22035.
- [112] K. D. G. I. Jayawardena, R. Rhodes, K. K. Gandhi, M. R. R. Prabhath, G. D. M. R. Dabera, M. J. Beliatas, L. J. Rozanski, S. J. Henley, S. R. P. Silva, *J. Mater. Chem. A* **2013**, 1, 9922.
- [113] J. Huang, Z. Yin, Q. Zheng, *Energy Environ. Sci.* **2011**, 4, 3861.
- [114] A. K. K. Kyaw, D. H. Wang, D. Wynands, J. Zhang, T.-Q. Nguyen, G. C. Bazan, A. J. Heeger, *Nano Lett.* **2013**, 13, 3796.
- [115] P. Cheng, H. T. Bai, N. K. Zawacka, T. R. Andersen, W. Q. Liu, E. Bundgaard, M. Jorgensen, H. Chen, F. C. Krebs, X. W. Zhan, *Adv. Sci.* **2015**, 2, 1500096.
- [116] N. Wu, Q. Luo, Z. W. Wu, C. Q. Ma, *Acta Phys. Chim. Sin.* **2015**, 31, 1413.
- [117] M. Krzywiecki, L. Grządziel, A. Sarfraz, D. Iqbal, A. Szwajca, A. Erbe, *Phys. Chem. Chem. Phys.* **2015**, 17, 10004.
- [118] S. Chen, C. E. Small, C. M. Amb, J. Subbiah, T.-H. Lai, S.-W. Tsang, J. R. Manders, J. R. Reynolds, F. So, *Adv. Energy Mater.* **2012**, 2, 1333.
- [119] M. Hartel, S. Chen, B. Swerdlow, H.-Y. Hsu, J. Manders, K. Schanze, F. So, *ACS Appl. Mater. Interfaces* **2013**, 5, 7215.
- [120] F. J. Lim, Y. T. Set, A. Krishnamoorthy, J. Ouyang, J. Luther, G. W. Ho, *J. Mater. Chem. A* **2015**, 3, 314.
- [121] Z. M. Kam, X. Z. Wang, J. Zhang, J. S. Wu, *ACS Appl. Mater. Interfaces* **2015**, 7, 1608.
- [122] B. A. MacLeod, B. J. T. de Villers, P. Schulz, P. F. Ndione, H. Kim, A. J. Giordano, K. Zhu, S. R. Marder, S. Graham, J. J. Berry, A. Kahn, D. C. Olson, *Energy Environ. Sci.* **2015**, 8, 592.
- [123] Z. Z. Shi, H. Liu, Y. P. Wang, J. Y. Li, Y. M. Bai, F. Z. Wang, X. M. Bian, T. Hayat, A. Alsaedi, Z. A. Tan, *ACS Appl. Mater. Interfaces* **2017**, 9, 43871.
- [124] J. S. Li, H. M. Jian, L. L. Yao, M. Zhao, J. Shu, X. W. Xiao, T. G. Jiu, *Sol. Energy* **2018**, 169, 49.
- [125] J. F. Wei, G. Q. Ji, C. J. Zhang, L. P. Yan, Q. Luo, C. Wang, Q. Chen, J. L. Yang, L. W. Chen, C. Q. Ma, *ACS Nano* **2018**, 12, 5518.
- [126] N. Wu, Q. Luo, Z. M. Bao, J. Lin, Y. Q. Li, C. Q. Ma, *Sol. Energy Mat. Sol. C* **2015**, 141, 248.
- [127] I. Ismail, J. Wei, X. Sun, W. Zha, M. Khalil, L. Zhang, R. Huang, Z. Chen, Y. Shen, F. Li, Q. Luo, C.-Q. Ma, *Sol. RRL* **2020**, 4, 2000289.
- [128] Y. L. Wang, L. P. Yan, G. Q. Ji, C. Wang, H. M. Gu, Q. Luo, Q. Chen, L. W. Chen, Y. Z. Yang, C. Q. Ma, X. G. Liu, *ACS Appl. Mater. Interfaces* **2019**, 11, 2243.
- [129] W. Zhao, L. Yan, H. Gu, Z. Li, Y. Wang, Q. Luo, Y. Yang, X. Liu, H. Wang, C.-Q. Ma, *ACS Appl. Energy Mater.* **2020**, 3, 11388.
- [130] H. Ma, H.-L. Yip, F. Huang, A. K.-Y. Jen, *Adv. Funct. Mater.* **2010**, 20, 1371.
- [131] R. Po, C. Carbonera, A. Bernardi, N. Camaioni, *Energy Environ. Sci.* **2011**, 4, 285.
- [132] M. P. de Jong, L. J. van IJzendoorn, M. J. A. de Voigt, *Appl. Phys. Lett.* **2000**, 77, 2255.
- [133] K. Norrman, N. B. Larsen, F. C. Krebs, *Sol. Energy Mat. Sol. C* **2006**, 90, 2793.
- [134] E. Vitoratos, S. Sakkopoulos, E. Dalas, N. Paliatsas, D. Karageorgopoulos, F. Petraki, S. Kennou, S. A. Choulis, *Org. Electron.* **2009**, 10, 61.
- [135] I. Irfan, A. J. Turinske, Z. Bao, Y. Gao, *Appl. Phys. Lett.* **2012**, 101, 093305.
- [136] Y. Yin, A. Sibley, J. S. Quinton, D. A. Lewis, G. G. Andersson, *Adv. Funct. Mater.* **2018**, 28, 1802825.
- [137] Y. Sun, C. J. Takacs, S. R. Cowan, J. H. Seo, X. Gong, A. Roy, A. J. Heeger, *Adv. Mater.* **2011**, 23, 2226.
- [138] W. Greenbank, L. Hirsch, G. Wantz, S. Chambon, *Appl. Phys. Lett.* **2015**, 107, 263301.
- [139] H. Zhang, A. Borgschulte, F. A. Castro, R. Crockett, A. C. Gerecke, O. Deniz, J. Heier, S. Jenatsch, F. Nüesch, C. Sanchez-Sanchez, A. Zoladek-Lemanczyk, R. Hany, *Adv. Energy Mater.* **2015**, 5, 1400734.
- [140] M. Ahmadpour, A. L. Fernandes Cauduro, C. Méthivier, B. Kunert, C. Labanti, R. Resel, V. Turkovic, H.-G. Rubahn, N. Witkowski, A. K. Schmid, M. Madsen, *ACS Appl. Energy Mater.* **2019**, 2, 420.
- [141] G. B. Adams, J. B. Page, O. F. Sankey, M. O'Keeffe, *Phys. Rev. B* **1994**, 50, 17471.
- [142] J. L. Segura, N. Martin, *Chem. Soc. Rev.* **2000**, 29, 13.
- [143] S. G. Stepanian, V. A. Karachevtsev, A. M. Plokhotnichenko, L. Adamowicz, A. M. Rao, *J. Phys. Chem. B* **2006**, 110, 15769.
- [144] P. C. Eklund, A. M. Rao, P. Zhou, Y. Wang, J. M. Holden, *Thin Solid Films* **1995**, 257, 185.
- [145] T. Kim, R. Younts, W. Lee, S. Lee, K. Gundogdu, B. J. Kim, *J. Mater. Chem. A* **2017**, 5, 22170.
- [146] C. H. Peters, I. T. Sachs-Quintana, W. R. Mateker, T. Heumueller, J. Rivnay, R. Noriega, Z. M. Beiley, E. T. Hoke, A. Salleo, M. D. McGehee, *Adv. Mater.* **2012**, 24, 663.
- [147] Z. Li, H. C. Wong, Z. Huang, H. Zhong, C. H. Tan, W. C. Tsoi, J. S. Kim, J. R. Durrant, J. T. Cabral, *Nat. Commun.* **2013**, 4, 2227.
- [148] Q. Burlingame, X. Tong, J. Hankett, M. Sliotzky, Z. Chen, S. R. Forrest, *Energy Environ. Sci.* **2015**, 8, 1005.
- [149] J. Wang, J. Enevold, L. Edman, *Adv. Funct. Mater.* **2013**, 23, 3220.
- [150] L. Yan, Y. Wang, J. Wei, G. Ji, H. Gu, Z. Li, J. Zhang, Q. Luo, Z. Wang, X. Liu, B. Xu, Z. Wei, C.-Q. Ma, *J. Mater. Chem. A* **2019**, 7, 7099.
- [151] Z. R. Li, J. K. Shan, L. P. Yan, H. M. Gu, Y. Lin, H. W. Tan, C. Q. Ma, *ACS Appl. Mater. Interfaces* **2020**, 12, 15472.
- [152] J. W. Arbogast, C. S. Foote, M. Kao, *J. Am. Chem. Soc.* **1992**, 114, 2277.
- [153] Z. R. Li, L. P. Yan, J. K. Shan, H. M. Gu, Y. Lin, Y. L. Wang, H. W. Tan, C. Q. Ma, *Energy Technol. Ger.* **2020**, 8, 2000266.
- [154] E. M. Speller, J. D. McGettrick, B. Rice, A. M. Telford, H. K. H. Lee, C.-H. Tan, C. S. De Castro, M. L. Davies, T. M. Watson, J. Nelson, J. R. Durrant, Z. Li, W. C. Tsoi, *ACS Appl. Mater. Interfaces* **2017**, 9, 22739.

- [155] Y. W. Soon, H. Cho, J. Low, H. Bronstein, I. McCulloch, J. R. Durrant, *Chem. Commun.* **2013**, 49, 1291.
- [156] S. Bertho, G. Janssen, T. J. Cleij, B. Conings, W. Moons, A. Gadisa, J. D'Haen, E. Goovaerts, L. Lutsen, J. Manca, D. Vanderzande, *Sol. Energy Mat. Sol. C* **2008**, 92, 753.
- [157] C. Zhang, T. Heumueller, S. Leon Cabanillas, W. Gruber, K. Burlafinger, X. Tang, J. D. Perea, I. Wabra, A. Hirsch, T. Unruh, N. Li, C. J. Brabec, *Energy Environ. Sci.* **2019**, 12, 1078.
- [158] D. E. Motaung, G. F. Malgas, C. J. Arendse, *J. Mater. Sci.* **2011**, 46, 4942.
- [159] X. Lu, H. Hlaing, D. S. Germack, J. Peet, W. H. Jo, D. Andrienko, K. Kremer, B. M. Ocko, *Nat. Commun.* **2012**, 3, 795.
- [160] C. Lindqvist, A. Sanz-Velasco, E. Wang, O. Bäcke, S. Gustafsson, E. Olsson, M. R. Andersson, C. Müller, *J. Mater. Chem. A* **2013**, 1, 7174.
- [161] J. Jo, S.-S. Kim, S.-I. Na, B.-K. Yu, D.-Y. Kim, *Adv. Funct. Mater.* **2009**, 19, 866.
- [162] A. Swinnen, I. Haeldermans, M. vande Ven, J. D'Haen, G. Vanhoyland, S. Aresu, M. D'Olieslaeger, J. Manca, *Adv. Funct. Mater.* **2006**, 16, 760.
- [163] S. Rafique, S. M. Abdullah, K. Sulaiman, M. Iwamoto, *Renewable Sustainable Energy Rev.* **2018**, 84, 43.
- [164] O. V. Mikhnenko, P. W. M. Blom, T.-Q. Nguyen, *Energy Environ. Sci.* **2015**, 8, 1867.
- [165] L. P. Yan, W. S. Zhao, Y. Z. Yang, H. Wang, X. G. Liu, C. Q. Ma, *Acta Polym. Sin.* **2021**, 52.
- [166] T. Heumueller, W. R. Mateker, I. T. Sachs-Quintana, K. Vandewal, J. A. Bartelt, T. M. Burke, T. Ameri, C. J. Brabec, M. D. McGehee, *Energy Environ. Sci.* **2014**, 7, 2974.
- [167] J. Yin, W. Zhou, L. Zhang, Y. Xie, Z. Yu, J. Shao, W. Ma, J. Zeng, Y. Chen, *Macromol. Rapid Comm.* **2017**, 38, 1700428.
- [168] C. Muller, *Chem. Mater.* **2015**, 27, 2740.
- [169] Z. Wang, H. Jiang, L. Zhang, X. Liu, J. Sun, Y. Cao, J. Chen, *Org. Electron.* **2018**, 61, 359.
- [170] K. H. Park, Y. J. An, S. Jung, H. Park, C. Yang, *ACS Nano* **2017**, 11, 7409.
- [171] K. H. Park, Y. An, S. Jung, H. Park, C. Yang, *Energy Environ. Sci.* **2016**, 9, 3464.
- [172] P. Yin, L. Wang, J. Liang, Y. Yu, L. Chen, C. Weng, C. Cui, P. Shen, *J. Mater. Chem. C* **2020**, 8, 11223.
- [173] P. Cheng, C. Q. Yan, T. K. Lau, J. Q. Mai, X. H. Lu, X. W. Zhan, *Adv. Mater.* **2016**, 28, 5822.
- [174] M. J. Xiao, K. Zhang, S. Dong, Q. W. Yin, Z. X. Liu, L. Q. Liu, F. Huang, Y. Cao, *ACS Appl. Mater. Interfaces* **2018**, 10, 25594.
- [175] H. Gu, L. Yan, Z. Li, J. Zhang, Q. Luo, Y. Yang, X. Liu, Z. Wei, C.-Q. Ma, *Sol. RRL* **2020**, 4, 2000374.
- [176] H.-C. Liao, C.-C. Ho, C.-Y. Chang, M.-H. Jao, S. B. Darling, W.-F. Su, *Mater. Today* **2013**, 16, 326.
- [177] S. J. Lou, J. M. Szarko, T. Xu, L. Yu, T. J. Marks, L. X. Chen, *J. Am. Chem. Soc.* **2011**, 133, 20661.
- [178] A. J. Pearson, P. E. Hopkinson, E. Couderc, K. Domanski, M. Abdi-Jalebi, N. C. Greenham, *Org. Electron.* **2016**, 30, 225.
- [179] W. Kim, J. K. Kim, E. Kim, T. K. Ahn, D. H. Wang, J. H. Park, *J. Phys. Chem. C* **2015**, 119, 5954.
- [180] B. J. T. de Villers, K. A. O'Hara, D. P. Ostrowski, P. H. Biddle, S. E. Shaheen, M. L. Chabiny, D. C. Olson, N. Kopidakis, *Chem. Mater.* **2016**, 28, 876.
- [181] N. Y. Doumon, M. V. Dryzhov, F. V. Houard, V. M. Le Corre, A. Rahimi Chatri, P. Christodoulis, L. J. A. Koster, *ACS Appl. Mater. Interfaces* **2019**, 11, 8310.
- [182] A. Classen, T. Heumueller, I. Wabra, J. Gerner, Y. K. He, L. Einsiedler, N. Li, G. J. Matt, A. Osvet, X. Y. Du, A. Hirsch, C. J. Brabec, *Adv. Energy Mater.* **2019**, 9, 1902124.
- [183] T. Heumueller, T. M. Burke, W. R. Mateker, I. T. Sachs-Quintana, K. Vandewal, C. J. Brabec, M. D. McGehee, *Adv. Energy Mater.* **2015**, 5, 1500111.
- [184] H. J. Cha, J. Y. Wu, A. Wadsworth, J. Nagitta, S. Limbu, S. Pont, Z. Li, J. Searle, M. F. Wyatt, D. Baran, J. S. Kim, I. McCulloch, J. R. Durrant, *Adv. Mater.* **2017**, 29, 1701156.
- [185] J. C. Blakesley, D. Neher, *Phys. Rev. B* **2011**, 84, 075210.
- [186] G. Garcia-Belmonte, P. P. Boix, J. Bisquert, M. Lenes, H. J. Bolink, A. La Rosa, S. Filippone, N. Martín, *J. Phys. Chem. Lett.* **2010**, 1, 2566.
- [187] Y. M. Wang, M. J. Jafari, N. N. Wang, D. P. Qian, F. L. Zhang, T. Ederth, E. Moons, J. P. Wang, O. Inganas, W. Huang, F. Gao, *J. Mater. Chem. A* **2018**, 6, 11884.
- [188] H. J. Schneider, *J. Am. Chem. Soc.* **1972**, 94, 3636.
- [189] Z. Bao, W. K. Chan, L. Yu, *J. Am. Chem. Soc.* **1995**, 117, 12426.
- [190] B. Carsten, F. He, H. J. Son, T. Xu, L. Yu, *Chem. Rev.* **2011**, 111, 1493.
- [191] J. A. Carr, K. S. Nalwa, R. Mahadevaparam, Y. Chen, J. Andereg, S. Chaudhary, *ACS Appl. Mater. Interfaces* **2012**, 4, 2831.
- [192] K. R. Graham, J. Mei, R. Stalder, J. W. Shim, H. Cheun, F. Steffy, F. So, B. Kippelen, J. R. Reynolds, *ACS Appl. Mater. Interfaces* **2011**, 3, 1210.
- [193] N. Camaioni, F. Tinti, L. Franco, M. Fabris, A. Toffoletti, M. Ruzzi, L. Montanari, L. Bonoldi, A. Pellegrino, A. Calabrese, R. Po, *Org. Electron.* **2012**, 13, 550.
- [194] A. Dupuis, P. Wong-Wah-Chung, A. Rivaton, J.-L. Gardette, *Polym. Degrad. Stab.* **2012**, 97, 366.
- [195] M. P. Nikiforov, B. Lai, W. Chen, S. Chen, R. D. Schaller, J. Strzalka, J. Maser, S. B. Darling, *Energy Environ. Sci.* **2013**, 6, 1513.
- [196] C.-Y. Chang, C.-T. Chou, Y.-J. Lee, M.-J. Chen, F.-Y. Tsai, *Org. Electron.* **2009**, 10, 1300.
- [197] H.-J. Lee, H.-P. Kim, H.-M. Kim, J.-H. Youn, D.-H. Nam, Y.-G. Lee, J.-G. Lee, A. R. B. Mohd Yusoff, J. Jang, *Sol. Energy Mat. Sol. C* **2013**, 111, 97.
- [198] J.-H. Kim, S. K. Park, J.-W. Lee, B. Yoo, J.-K. Lee, Y.-H. Kim, *J. Korean Phys. Soc.* **2014**, 65, 1448.
- [199] M. D. Clark, M. L. Jespersen, R. J. Patel, B. J. Leever, *Org. Electron.* **2014**, 15, 1.
- [200] J. Won Lim, C. Kyu Jin, K. Yong Lim, Y. Jae Lee, S.-R. Kim, B.-I. Choi, T. Whan Kim, D. Ha Kim, D. Kyung Hwang, W. Kook Choi, *Nano Energy* **2017**, 33, 12.
- [201] I. A. Channa, A. Distler, M. Zaiser, C. J. Brabec, H.-J. Egelhaaf, *Adv. Energy Mater.* **2019**, 9, 1900598.
- [202] S. J. Sung, J. Park, Y. S. Cho, S. H. Gihm, S. J. Yang, C. R. Park, *Carbon* **2019**, 150, 275.
- [203] A. Morlier, S. Cros, J.-P. Garandet, N. Alberola, *Sol. Energy Mat. Sol. C* **2013**, 115, 93.
- [204] D. Angmo, S. A. Gevorgyan, T. T. Larsen-Olsen, R. R. Søndergaard, M. Hösel, M. Jørgensen, R. Gupta, G. U. Kulkarni, F. C. Krebs, *Org. Electron.* **2013**, 14, 984.
- [205] G. Dennler, C. Lungenschmied, H. Neugebauer, N. S. Sariciftci, M. Latrèche, G. Czeremuszkin, M. R. Wertheimer, *Thin Solid Films* **2006**, 511–512, 349.
- [206] D. Angmo, P. M. Sommeling, R. Gupta, M. Hösel, S. A. Gevorgyan, J. M. Kroon, G. U. Kulkarni, F. C. Krebs, *Adv. Eng. Mater.* **2014**, 16, 976.
- [207] H. C. Weerasinghe, D. Vak, B. Robotham, C. J. Fell, D. Jones, A. D. Scully, *Sol. Energy Mat. Sol. C* **2016**, 155, 108.



**Lingpeng Yan** obtained a Ph.D. degree in materials science and engineering from Taiyuan University of Technology in 2017. He is now an associate researcher at Taiyuan University of Technology and a postdoctoral researcher at Suzhou Institute of Nano-Tech and Nano-Bionics (SINANO) Chinese Academy of Sciences (CAS). His research interests are focused on the stability of organic solar cells and synthesis and application of carbon nanomaterials.



**Chang-Qi Ma** received his Ph.D. degree at the Technical Institute of Physics and Chemistry, CAS in Beijing. After that he was a postdoctoral research assistant at Heriot-Watt University in Edinburgh, UK, then he joined the research group of Professor Peter Bäuerle at the University of Ulm in 2004 as a Humboldt research fellow. From 2007 to 2011, he did his Habilitation at the Institute of Organic Chemistry II and Advanced Materials, Ulm University. In June 2011 he joined SINANO, CAS, as a professor. His research interests include: synthesis of organic/inorganic semiconductors, printing processing, degradation and stability of organic/perovskite Solar Cells.